IEEE Access
Multidisciplinary | Rapid Review | Open Access Journal

Received 18 September 2023, accepted 8 October 2023, date of publication 12 October 2023, date of current version 26 October 2023.

Digital Object Identifier 10.1109/ACCESS.2023.3324130

RESEARCH ARTICLE

Collaborative Layout Optimization for Ship Pipes Based on Spatial Vector Coding Technique

HONGSHUO ZHANG[1], MINGJUN YANG[1], YUANSONG YANG[2], HAIYANG LIU[2], AND YAN LIN[1]
[1]School of Naval Architecture and Ocean Engineering, Dalian University of Technology, Dalian 116024, China
[2]Science and Technology on Green Construction Laboratory, China Nuclear Industry 23 Construction Company Ltd., Beijing 101300, China

Corresponding author: Hongshuo Zhang (15103255157@163.com)

This work was supported in part by the Development Fund of the Science and Technology on Green Construction Laboratory, China National Nuclear Corporation (CNNC), under Grant CNNC-STGCL-KFKT-2022-001.

ABSTRACT Ship Pipe Route Design (SPRD) has always been a challenging and critical aspect in the detailed design for various types of ships. However, existing layout methods are inefficient, existing algorithms lack consideration for collaborative layouts in practical engineering, true intelligent design has not yet been achieved, and the issue of collaborative layout of pipes has been insufficiently researched. Based on the aforementioned research status, this paper proposes a novel collaborative pipe layout method. Firstly, a high-dimensional vector encoding technique to innovate the underlying mathematical representation of pipes is proposed, breaking free from traditional constraints. Secondly, a powerful and engineering-applicable hybrid AA-SPOP algorithm is incorporated, which is based on the heuristic swarm intelligence algorithm known as Artificial Fish Swarm Algorithm (AFSA), exhibits advantages such as high global optimization efficiency and strong adaptability. To mitigate potential issues like suboptimal local optimization and high sensitivity, this paper proposes a parameter adaptive equation and a series of optimization adjustment. Thirdly, a collaborative pipe layout method that considers support equipment is proposed. This paper effectively addresses the lack of research in this area by introducing branch pipe collaboration methods and energy zone guidance methods. Finally, through engineering simulation experiments, the paper demonstrates the efficiency, feasibility, and cutting-edge nature of the proposed collaborative layout optimization method.

INDEX TERMS Heuristic hybrid algorithm, ship pipe and equipment collaborative layout optimization, ship pipe route design (SPRD), vector encoding technique.

I. INTRODUCTION

The piping system of ships, resembling a complex orthogonal spider web, serves as a core system for transporting various substances such as water, oil, and natural gas required for ship operation and living areas. The Ship Pipe Route Design (SPRD) is crucial for ensuring the safety of the entire ship, particularly in terms of the coordinated design of the overall pathway [1]. SPRD is typically carried out during the detailed design phase of ship construction [2], requiring a comprehensive consideration of factors such as structural spatial constraints and system functionality specific to ships [3]. Over the past few decades, optimizing the layout of ship pipe systems has been a significant research topic in the field of shipbuilding. Despite the continuous iteration and advancement of numerous optimization methods, human factors still play a significant role in the process. In recent years, with the continuous development of computer technology and increasing concerns about energy efficiency and environmental impact, the study of piping collaborative layout in ships has become increasingly important. By implementing rational design and optimizing the layout of the piping system, it is possible to maximize the performance of ships.

A. RECENT RESEARCH

Since the mid-20th century, scholars have conducted extensive research on optimization of ship pipe routing. This

The associate editor coordinating the review of this manuscript and approving it for publication was Amjad Ali.

includes pipe path encoding methods, pipe path optimization algorithms, and collaborative layout among multiple pipes.

1) RESEARCH ON ENCODING TECHNIQUES AND OPTIMIZATION ALGORITHMS

Currently, the algorithms involved in pipe layout design mainly consist of deterministic algorithms, heuristic algorithms, and hybrid or enhanced algorithms. Deterministic algorithms (such as Dijkstra [4], A $*$ [5], and line search methods [6]) search for globally optimal pipe paths based on the properties of the layout. They exhibit high computational efficiency but lack diversity and innovation. Moreover, they generally rely on grid spaces, which increase the difficulty of preprocessing and computational memory requirements. Heuristic algorithms, in comparison to deterministic algorithms, obtain multiple solutions through random searches and iterations [7]. These include evolutionary intelligence algorithms like Genetic Algorithm (GA) [8], Differential Evolution Algorithm (DE) [9], and swarm intelligence algorithms like Ant Colony Optimization (ACO) [10], Particle Swarm Optimization (PSO) [11], Whale Optimization Algorithm [12], among others. However, these algorithms are sensitive to parameter settings, may converge to local optima, and have higher requirements for pipe encoding methods. Hybrid or enhanced algorithms combine the advantages of the previous two types, such as GA-A* [13], MA-NSGA-II [14] and IDAACO [15]. However, existing research has found that hybrid algorithms based on traditional grid encoding methods may not be well suited for irregular shapes and complex problems.

In recent years, heuristic swarm intelligence algorithms have demonstrated significant advantages in pipe layout [16], particularly the Artificial Fish Swarm Algorithm (AFSA) [17], which has shown superiority compared to other heuristic algorithms. Huang et al. [18] successfully applied AFSA to robot path planning, while Zhang et al. [19] utilized it in the path planning of Autonomous Surface ships. Practical applications have shown that AFSA possesses the global search capability of GA, the fast optimization ability of PSO, and the adaptability and robustness of ACO.

Currently, the optimization algorithms used for SPRD, especially heuristic algorithms, typically rely on grid spaces [20], [21], [22]. This obviously increases the difficulty of layout space preprocessing, consumes significant memory and time, and cannot be applied to layouts with irregular shapes. However, most existing pipe encoding methods mainly adopt grid-based encoding and lack efficient and concise dedicated pipe layout encoding methods. This limitation hinders the efficient use of hybrid algorithms in handling complex ship pipe layouts, as they cannot provide sufficient flexibility and adaptability. Currently, a considerable number of non-grid encoding methods have emerged in various fields [23], [24], [25], [26]. In light of the shortcomings of existing encoding methods for pipes, this paper pioneers a new and highly practical encoding approach that overcomes these limitations and offers enhanced utility.

2) RESEARCH ON COLLABORATIVE LAYOUT OPTIMIZATION

The collaborative layout design of pipes primarily focuses on the coordinated design of main and side branch pipes, or the mixed collaboration design of multiple different types of pipes. In actual ship pipes, over half of the quantity comprises branch pipes [27], which interact with and constrain each other. Currently, optimization methods for branch pipe layout include the straight branch method [28] and the problem decomposition method [29]. The main principle is to decompose the branch pipe system into multiple individual pipes and further optimize them by setting energy influence parameters and employing different collaborative algorithms. However, an analysis reveals that the aforementioned methods still have some issues, such as dependence on grid-based spaces and susceptibility to local optima. Therefore, researching a suitable branch collaboration method is crucial for the layout of mixed pipes.

In ship pipe layout problems, in addition to considering the collaboration between pipes, it is also important to consider the collaborative layout between pipes and support equipment. Some researchers have studied this aspect [30], [31], generally focusing on optimizing support equipment based on factors such as pipe stress, resistance, and material analysis. However, there is still a lack of feasible approaches to achieve the optimal integration of both objectives, and the research is still inadequate.

B. ARTICLE INNOVATION AND SIGNIFICANCE

This article addresses the bottleneck issues in the field of SPRD and proposes a novel ship pipe collaborative layout optimization method. The innovations and improvements of the proposed method can be summarized in the following three aspects.

First, in terms of mathematical representation of pipes, a high-dimensional vector encoding method tailored to pipe characteristics has been proposed. It breaks away from the limitations of traditional grid-based encoding approaches.

Second, in terms of optimization algorithms, a hybrid heuristic swarm intelligence algorithm called AA-SPOP is introduced based on the vector encoding. This algorithm is capable of providing more precise and diversified collaborative layout solutions, significantly improving the efficiency of SPRD and making it more intelligent.

Third, addressing the current research gap in collaborative layout within the pipe domain, novel collaborative optimization methods are proposed to address the challenges of mixed-type pipe collaboration and pipe equipment collaboration. These include the vector projection branch method and the energy-guided optimization method for support equipment. These approaches contribute valuable insights to this field.

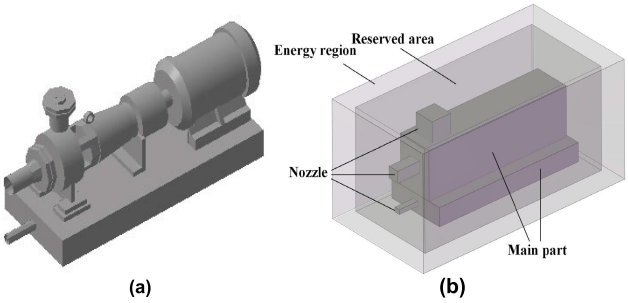

FIGURE 1. The example of rectangular envelope processing. (a) Before envelope processing. (b) After envelope processing.

Through these innovative improvements, a new pipe collaborative layout mechanism is established, providing a new perspective for the SPRD and making a novel contribution to the field of pipe collaborative layout.

II. SPRD FORMULATION

A. MATHEMATICAL ANALYSIS OF LAYOUT SPACE

Pipes are distributed throughout various parts of a ship, particularly in the cabin of ships. The layout of the pipe system must make efficient use of limited space and be coordinated with other equipment, compartments, and structures to avoid interference or conflicts. SPRD primarily involves designing the entire ship's piping system within a limited three-dimensional space, following specific engineering specifications and optimization objectives.

Before designing pipe layouts, it is essential to conduct research and analysis of the layout space to understand the locations of pipe interfaces and the layout requirements for various areas within cabin. In the layout space, equipment is generally considered as obstacles or infeasible areas. To describe the geometric shapes of these obstacles, a subdivision rectangular enveloping method is used for approximate modeling. This method is widely applied due to its simplicity in calculation and high accuracy of representation [32]. It mainly involves constructing a combination of rectangular envelopes for different areas of the equipment, such as the main body area, interface area, and reserved area. The illustration below (Fig. 1) demonstrates this concept.

The layout environment and equipment of ships are special, and certain areas in the layout space often favor or exclude the placement of pipes. To address this, different energy zones are defined to guide the desired path of ship pipes, ensuring that the pipe layout meets safety, operational, and efficiency requirements. The concept of energy zones is similar to the rectangular enveloping method, primarily enveloping the areas around equipment or structures. These energy zones are virtually defined as square spaces based on pipe design specifications. Table 1 illustrates the main aspects considered, including guiding and exclusionary regions, within these energy zones.

TABLE 1. Energy zone setting specifications.

Objective	Specification Requirements
Support fixation	Preferably aligned along bulkheads, equipment surfaces, and floors.
Pipe collaborative	High degree of overlap and parallelism for branch pipes
Physical attributes	Balancing of pressure, temperature, and flow velocity regions.
Specific spaces	Avoid safe passageways, work areas, roads, special equipment (electrical, electronic, communication equipment, etc.), etc., and pass through piping support equipment.

B. HIGH-DIMENSIONAL VECTOR ENCODING METHOD FOR SPRD

Currently, the most widely used method for analyzing pipe layout is the grid-based approach. However, this method has several limitations, such as limited discrete accuracy, spatial layout distortion, high time cost, and difficulties in grid precision division. To address these issues, this paper proposes a novel pipe encoding technique called Spatial High-Dimensional Vector Encoding, which is characterized by its simplicity, universality, flexibility, and continuous processing. The detailed principles of the high-dimensional vector encoding are as follows:

1) PREPROCESSING OF LAYOUT SPACE

The grid-based method primarily involves the discretization of regular spatial structures. It presents challenges in selecting an appropriate grid precision, requires lengthy preprocessing, and faces difficulties in dealing with irregular shapes in continuous spaces. Additionally, path optimization can only occur along grid trajectories. Fig. 2 illustrates a comparison between the grid-based method and the approach presented in this paper (taking the xy-plane as an example, with a grid precision assumed to be 1). In Fig. 2(a) and (b), 1 represents regular feasible regions, 0 and 2 represent infeasible regions, and black dots denote the starting and ending points of paths. Fig. 2(a) depicts a regular rectangular space, but the red path along the digit 2 is an irregular diagonal path, which does not conform to the grid-based principle. Fig. 2(b) shows an irregular elliptical space, where the region marked by 0 is typically located at the edges or outside of irregular spaces. As indicated by the red region, the solution accuracy is compromised at the spatial edges, preventing accurate arrival at the target point.

In contrast, the vector-based approach imposes no limitations on the shape of the layout space and is suitable for irregular spatial shapes such as triangular prisms, trapezoidal

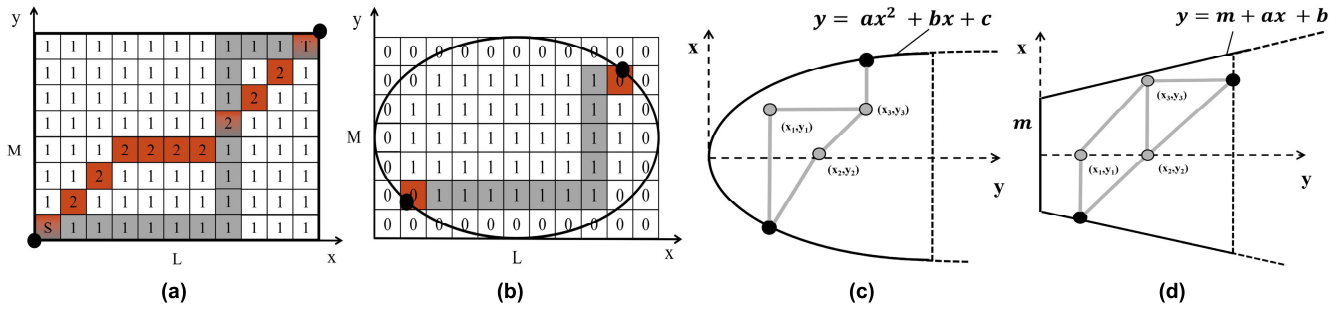

FIGURE 2. Comparison of path optimization results using different encoding methods. (a) Regular space (grid encoding). (b) Irregular space (grid encoding). (c) Irregular space (vector encoding) 1. (d) Irregular space 2 (vector encoding).

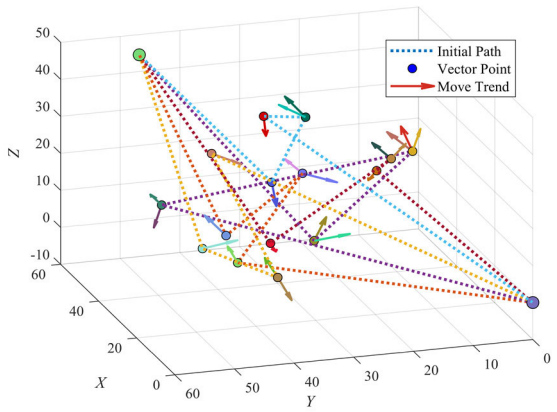

FIGURE 3. Example of the principle of spatial vector encoding.

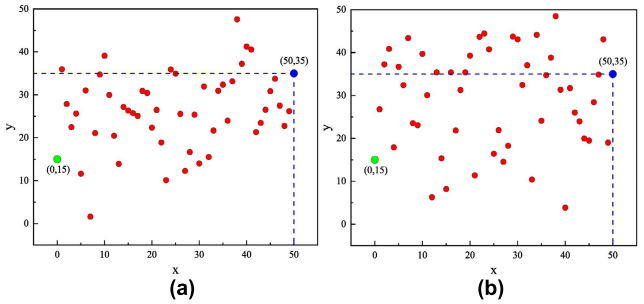

FIGURE 4. Principle of vector initialization. (a) Gaussian distribution. (b) Random distribution.

prisms, and others. The entire spatial layout is primarily characterized using multidimensional x, y, and z vectors, representing the coordinates of pipe path nodes and the positions and shapes of various spatial components. It avoids the issue encountered by grid-based methods, where paths must be optimized along grid trajectories. As shown in Fig. 2(c) and (d), for two irregular spaces, the xy coordinate vectors only need to satisfy the prescribed Equation (1), where a, b, and c are constant parameters. Vector points can be located anywhere in space and are not constrained by grids. They can follow diagonal or straight paths and various other trajectories. Multiple paths can be generated by connecting vector points.

$$\begin{cases} y = ax^2 + bx + c \\ y = m + ax + b \end{cases} \tag{1}$$

2) MATHEMATICAL EXPRESSION

To optimize the representation of piping path, and meet engineering specifications, a novel encoding method for is proposed, mathematically expressed as shown in Equation (2). This includes the starting point S, a list of vector points V, and the endpoint E. As per the equation, the high-dimensional vector list comprises coordinate vectors x_i, y_i and z_i(i = 1, 2, ... n), as well as constraint vectors f and l. Coordinate vectors represent the coordinates of points along the path, where each (x_i, y_i, z_i) forms a three-dimensional coordinate vector point representing the path nodes. Vectors f and l control each coordinate vector point, providing auxiliary guidance for algorithm optimization. It's important to note that f and l vectors are not visually represented in space but actively participate in the calculations among coordinate vector points, thereby optimizing the path trajectory. The principles of coordinate vectors and control vectors will be elaborated upon below.

The initial values of coordinate vector points are systematically generated based on the shape, range, and the positions of the pipe's start and end points within the layout space. Through analysis and validation, it has been determined that Gaussian distribution is an effective method for generating these initial values. Fig. 4 illustrates a comparative test between the Gaussian distribution method and the conventional random method (with the same start and end points). By adjusting the mean and standard deviation, the initial positions of vector points can be controlled within the desired range effectively. Using this method, a series of coordinate vector points in three-dimensional space is generated, along with the initial configuration of paths, as shown in Fig. 3 (the colors are only for distinguishing each path and their associated coordinate vector points). From the figure, it can be observed that a series of coordinate vector points are generated within the square space, along with their initial movement trends. Initial paths can be generated by connecting the vector points, and subsequent optimization of

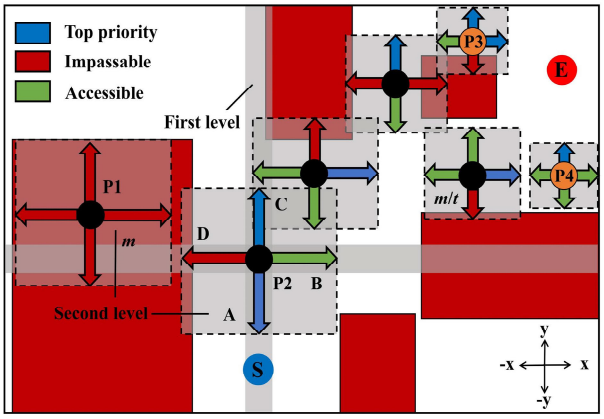

FIGURE 5. The example of Cross-Guiding process.

coordinate vector points results in the desired path. This method, in contrast to grid encoding, is not constrained by grids or spatial limitations.

$$Pipe = \{S, V, E\} \tag{2a}$$

$$V = [(x_1, y_1, z_1, f_1, l_1), \cdots, (x_n, y_n, z_n, f_n, l_n)] \tag{2b}$$

The roles of control vectors f and l differ, with f acting as a constraining factor and l as a guiding factor. The fundamental principles underlying these roles are analyzed as follows:

The main role of control vector l is to constrain the movement between individual coordinate vector points. Equation (3) calculates the Manhattan distance $|l_n l_{n-1}|$ between connecting points, ensuring compliance with the minimum distance requirement (100mm) as per engineering standards. Equation (4) enforces the constraint that three adjacent vector connection points cannot be collinear, with n denoting the label of each point and m representing the maximum point. It is important to note that this equation is applicable when the start and end points are on different planes, effectively reducing computational complexity.

$$|l_n l_{n-1}| = |x_n - x_{n-1}| + |y_n - y_{n-1}| + |z_n - z_{n-1}| \tag{3}$$

$$0° < \left(\frac{180}{\pi}\right) \cos^{-1}\left(\frac{l_n l_{n-2}}{|l_n|\,|l_{n-2}|}\right) < 180°, n = 3, 4 \cdots m \tag{4}$$

Another control vector, f, is the Cross-Guidance Vector, which determines the quality of coordinate vector points by assessing orthogonal plane obstacles. This control vector enhances the precision and speed of global optimization. The approach involves a two-tier cross-guidance range search for each coordinate vector point along six orthogonal extension directions: x, -x, y, -y, z, and -z. Using point P2 in the xy-plane as an example, as illustrated in Fig. 5, there are two levels of search assessments (highlighted in the gray area). After the first-tier global assessment, it is evident that direction AC is unobstructed across the entire global search range, designating it as the optimal feasible direction, resulting in a corresponding increase in the overall fitness value by $n \times H$. Here, n denotes the number of feasible directions, and H represents the guidance value. Following the second-tier local assessment within the $m \times m$ range (with m set at 10% of the spatial extent), it was observed that direction D encountered an obstacle, resulting in a reduction of the overall fitness value by $n \times F$, where F represents the decay factor. To ensure both precision and stability in the algorithm, the value of m adheres to the formula $m = m/t$, where t denotes the number of iterations. In this study, values of H and F are chosen to be around ± 100.

C. CONSTRAINTS AND EVALUATION FUNCTION

Pipe layout design for ships should consider the layout environment and engineering design background, along with understanding the optimization objectives and constraints of pipe paths [33]. In order to meet the requirements of different engineering backgrounds for pipe layout design, a comprehensive evaluation should be conducted from multiple perspectives. The main summary of optimization objectives, constraints, and the design of evaluation functions in this study is as follows:

1) OPTIMIZATION OBJECTIVES AND CONSTRAINTS

The optimization objectives for pipe layout are as follows:

(1) Minimize the length of the path.

(2) Minimize the number of elbows in the pipe, while adhering to the minimum bending requirements.

(3) Optimize the placement of the pipe to comply with the requirements of the energy zones, ensuring proximity to bulkheads, equipment, etc., and avoiding restricted areas.

(4) Parallel layout of closely spaced pipes of the same type.

(5) Consider different operational conditions and requirements of the ship, such as load and temperature variations, to ensure safety.

Due to the special layout environment of ship, there are various constraints on pipe placement, primarily based on the ship's structural design, cabin layout, and regulatory requirements. The specific constraints can be summarized as follows:

(1) Prohibition of pipe paths through obstacles, such as hull structure, equipment, existing pipes, and reserved spaces.

(2) Pipe paths must be perpendicular or parallel to the cabin spaces and equipment, and each adjacent sub-path must be either perpendicular or collinear (meeting orthogonality). Engineers have the flexibility to adjust these factors in practical engineering.

(3) Adequate safety clearance should be maintained between the pipe and special equipment, structures, or other pipes to facilitate operation and maintenance. The distance between adjacent elbow points should not be less than the specified length.

$$\min_{x \in D} f(x) = [f_1(x), f_2(x), \cdots, f_k(x)]^T \tag{5a}$$

$$s.t. \begin{cases} g_i(x) \le 0, i = 1, \cdots m \\ h_j(x) = 0, j = 1, \cdots n \end{cases} \tag{5b}$$

2) DESIGN OF THE EVALUATION FUNCTION

The design of the objective evaluation function follows the mathematical expression commonly used for multi-objective optimization problems (as given in Equation (5)). It represents the extreme value objective of a function that is constrained by multiple inequality or equality variables. SPRD is a multi-objective optimization problem, considering the requirements for cost-effectiveness, efficiency, and safety of the pipe layout. In order to achieve the optimal overall values for these objectives, a comprehensive and accurate evaluation function is established as shown in Equation (6), where a negative sign is introduced to transform the minimization problem into a maximization problem, where W is a large positive constant.

$$F_{\max}(path(v)) = W - (p_1 \times Orth(v) + p_2 \times Obs(v) + p_3 \times Lenth(v) + p_4 \times Elbow(v) - p_5 \times Power(v) - p6 \times F\_L(v)) \quad (6a)$$

$$s.t.g(p) = 0, h(p) = 0, v \in bound \quad (6b)$$

The concepts of each sub-objective function are as follows, the values of p_1 to p_6 correspond to the weight parameters of each objective. v denotes the coordinate vector point.

(1) $Orth(v) = \sum_{i=1}^{N} O(v_i, v_{i+1})$ represents the non-orthogonality degree between path connection points.

(2) $Obs(v) = \sum_{i=1}^{N} S(v_i, v_{i+1}, obslist)$ represents the intersection degree between path connection points and obstacles or restricted areas.

(3) $Lenth(v) = \sum_{i=1}^{N} L(v_i, v_{i+1})$ represents the total length of the pipe path.

(4) $Elbow(v)$ represents the number of bending points required for the pipe path.

(5) $Power(v) = \sum_{i=1}^{N} P(v_i, v_{i+1}, powerlist)$ represents the length of the path passing through the energy zone indicates its desirability, with larger values being more favorable. In the function, the negative symbol is used to denote this guiding value.

(6) $F\_L(v) = \sum_{i=1}^{N} (F(v_i, obslist) + L(v_i, v_{i+1}, v_{i+2}))$ represents the quality of the position of the path's vector points, primarily serving a guiding role to ensure algorithm efficiency and accuracy.

The multi-objective optimization problem can be transformed into a single-objective optimization problem by assigning a series of weight coefficients. The weight values can be adjusted based on the importance of each objective to generate multiple solutions. Through experimental research on parameter normalization, it has been found that the pipe layout achieves optimal results when the weight coefficients p_1-p_6 approximate the following proportion: 1: 10: 0.001: 1: 0.5: 0.1.

III. AA-SPOP ALGORITHM

A. AFSA ALGORITHM

The Artificial Fish Swarm Algorithm (AFSA) is a population-based intelligent optimization algorithm that simulates the preying and migration behaviors of fish populations [14]. It is generally used for problems with a large population size (or initial vector size) and achieves optimization through the coordinated behavior of fish. The algorithm involves four main parameters: perception range (*Visual*), search step length (*Step*), congestion factor (δ), and number of search attempts (*Try_number*). Assuming there are N artificial fish, each fish's state can be represented as a vector $X_m = (x_1, x_2, \cdots x_n), m = 1, 2 \cdots N$, where $x_i (i = 1, 2, \cdots, n)$ represents each optimization variable of the artificial fish. An adaptive function $Y = f(X)$ is designed to represent the food concentration, where Y represents the objective function value.

The AFSA algorithm consists of four main behaviors (original equations can be found in reference [14]):

1) Preying behavior: Search for artificial fish with better fitness values within the visual range and move towards them.

2) Swarming behavior: Decide whether to move towards the center position based on the fitness of neighboring artificial fish and the richness of food at the center.

3) Following behavior: Adjust one's own movement direction based on the optimal solution in the nearby range and conduct local search.

4) Random behavior: When a better solution cannot be found within the visual range, randomly move a step length to increase the diversity of the search process.

B. AA-SPOP ALGORITHM PRINCIPLE

While the AFSA algorithm boasts several advantages, its application to pipe routing optimization reveals a number of evident issues, such as susceptibility to local optima, unstable convergence performance, and sensitivity to parameters, among others. In response to these challenges, this paper introduces performance enhancements, such as adaptive parameter strategies and a staged optimization approach, resulting in the proposed AA-SPOP algorithm. Its workflow is illustrated in Fig. 8. Detailed descriptions of the enhancements in each part are as follows:

1) DESIGN OF PARAMETER ADAPTATION EQUATIONS

Although the AFSA algorithm converges quickly, it is highly sensitive to the settings of parameters such as the *Visual*, *Step*, and δ. These parameters constitute the core of the algorithm's optimization procedures. Consequently, the algorithm struggles to strike a balance between optimization speed and precision, leading to susceptibility to local optima, particularly in later stages, characterized by oscillatory behavior. As shown in Fig. 6, in the later phases of the algorithm, it may converge around the global optimal solution, *Ideal goal*. However, due to excessively large *Step* and *Visual* values, it may continuously search for suboptimal solution, *Real goal*, in the vicinity and fail to find the precise solution.

Therefore, addressing the aforementioned issues, this paper proposes three adaptive adjustment formulas as follows. The corresponding decay curves are illustrated in Fig. 7, where x represents the current iteration count, and y represents the degree of decay. The parameters *Visual*, *Step*, and δ

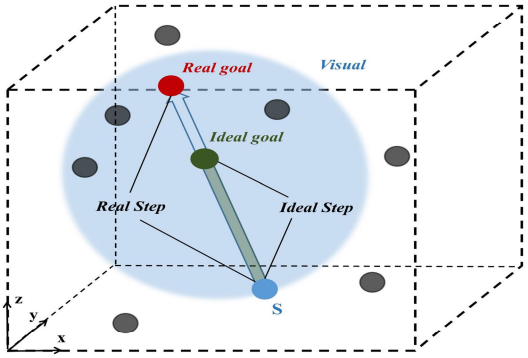

FIGURE 6. Optimization process of the AFSA algorithm.

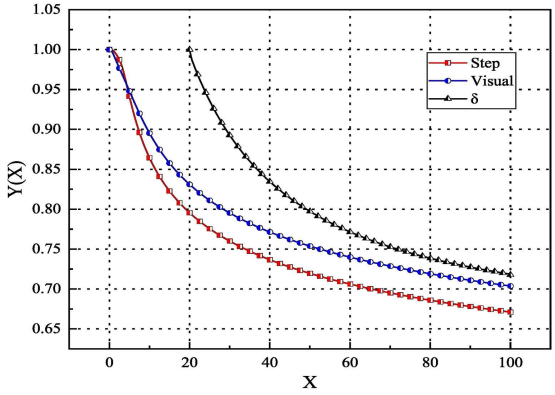

FIGURE 7. The decay curve of the adaptive equations.

directly influence the algorithm's convergence performance. Taking the maximization problem as an example, a larger δ indicates a smaller allowed crowding degree, which enhances the ability of artificial fish to escape from local optima but leads to slower convergence speed. Larger *Visual* and *Step* values can quickly converge to the vicinity of the global optimum. However, in the later phase, they struggle to achieve an accurate solution.

$$k = \left(\frac{1}{1 + a \times (x - b)^c}\right)^n \tag{7a}$$

$$y = \frac{1}{1 + a \times \log_{10}\left[1 + \left(\frac{x-b}{k}\right)^c\right]} \tag{7b}$$

To ensure the algorithm's comprehensive optimization capabilities throughout the entire iteration cycle, an adaptive decay equation (Equation (7) for *Visual* and *Step*, and Equation (8) for δ) is proposed. In Equation (7), parameter a mainly controls the initial descent rate, while parameter b represents the initial value for iteration. Parameter c primarily governs the descent range, and experimental results suggest *Visual* is around 3 and *Step* is around 5. Parameter k controls the shape of the descent curve, and it has been found that *Visual* exhibits optimal performance with the exponent n is set to 2, while *Step* achieves optimal results with the exponent n of 3. In Equation (8), the parameter x_t represents the starting generation for decay. Through multiple experimental analyses, the parameter k controls the decay rate and is set to approximately 30. The parameter P controls the shape of the decay curve and is set to around 1. δ_0 represents the initial maximum value, while δ_e represents the final value.

$$\delta_t = \delta_e + \frac{\delta_0 - \delta_e}{1 + \left(\frac{x - x_t}{k}\right)^p} \tag{8}$$

2) PHASED OPTIMIZATION AND PSO OPERATIONS

During the process of optimizing ship pipe routing, the AFSA algorithm exhibits inconsistency between its early and late phases, posing challenges in controlling the stability and robustness of algorithm convergence. To address this issue, a phased optimization strategy is proposed in this paper based on the AFSA algorithm, which comprises two tiers of phased operations: global iterations and local behaviors. Furthermore, in the initial phase, the concept of Particle Swarm Optimization (PSO) is introduced to further enhance the algorithm's convergence speed [9]. The specific principles are explained as follows:

a: PHASED OPTIMIZATION STRATEGY

Phased optimization involves two aspects (Fig. 8). On the one hand, the entire iterative cycle is divided into two phases. Through repeated experimental testing, the algorithm typically converges to the vicinity of the optimal solution at approximately $0.15 \times T$ iterations. Consequently, the division of early and late phases is determined using $0.15 \times T$ as the benchmark, where T represents the number of iterations. The early phase combines adaptations of the PSO algorithm, while the later phase reverts to the basic equation of the AFSA algorithm. On the other hand, it divides the swarming and following behaviors into different phases, with the main segmentation point set at $40\% \times N$, where N represents the initial population size.

In the early phases of iteration, the swarming behavior can be divided into two phases. In the first phase (adjacent individual less than $40\% \times N$), due to low crowding and low food concentration, an adjustment is made by increasing $\delta \times Y$, which corresponds to increasing the crowding restriction. This adjustment is implemented to prevent individual from moving towards suboptimal positions. The second phase indicates a higher crowding degree, suggesting proximity to the optimal position. Here, δ remains constant, and normal swarming behavior is conducted. However, as individuals are now clustered around the optimal solution, a reduction in movement speed of approximately 10% is implemented to ensure algorithm stability.

The following behavior has a greater impact on the algorithm's convergence. Therefore, in the phases of the early iterations, δ needs to be reduced and crowding restrictions increased, allowing movement only towards highly promising individual. The moving speed in the second phase should be significantly reduced to effectively avoid being trapped in local optima due to continuous following of suboptimal

individual. In the phases of the later iterations, δ is slightly increased to ensure convergence performance and escape from local optima to search for the precise optimal solution.

b: OVERVIEW OF PSO ALGORITHM OPERATIONS

According to Fig. 8, in order to provide effective guidance in the early phases, the PSO algorithm is introduced by incorporating individual best positions (*pbest*) and global best position (*gbest*) parameters. The four behavior equations of the fish swarm algorithm are modified to better guide the search towards the global optimum. In the later iterations, the original operations of the AFSA algorithm are used to ensure stability. Additionally, a global guidance operation similar to PSO algorithm is incorporated after the completion of each major step in the algorithm. The specific modified equations are shown in Equations (9) to (13), at the bottom of the page, where c_1 and c_2 represent local and global parameters, respectively. *Randn* and *RandStep* denote random numbers and random step lengths, respectively. X_c and $X_{\max}$ respectively represent the central value and maximum value of the neighboring population region, denotes the maximum value in the surrounding search, with n_f representing the number of surrounding individuals. F is the global decay factor, W denotes the inertia weight of the PSO algorithm, t and T represent the current and maximum iteration counts, respectively. *Tag* refers to the best solution found.

3) STABILITY OPTIMIZATION OPERATION

Although corresponding improvement strategies have been implemented for both early and late phases of the algorithm, it is undeniable that unstable results may still occur under certain special or occasional circumstances. To enhance the algorithm's robustness and optimization precision, several optimization operations are proposed, outlined as follows:

a: RANDOM ELIMINATION OPERATION

As depicted in Fig. 8, the elimination strategy is carried out after each individual completes the primary algorithmic operations. This operation primarily aims to reduce the algorithm's variability. It involves sorting and comparing all artificial fish based on their fitness values (Y_i) and eliminating the least performing individuals, with vacant positions being replenished in a manner akin to mutation. After experimental validation and analysis, the following two strategies were identified for different phases of iteration:

$$X_{new} = n_1 \times X_{best1} + n_2 \times (X_{best2} - X_{best3}) \tag{14a}$$

$$n_1 + n_2 \le 1, n_1 \ge n_2 \tag{14b}$$

Elimination Strategy 1: Taking the elimination of one individual as an example, the three individuals with the highest fitness values are selected, and a new individual is generated using the following Equation (14).

$$X_{new} = mutation\left(X_{fill}, pmutation, sigma\right) \tag{15a}$$

$$sigma = s \times (bound_{\max} - bound_{\min}) \tag{15b}$$

$$0.15 \le pmutation \le 0.2 \tag{15c}$$

Elimination Strategy 2: This approach mainly utilizes Gaussian mutation, as shown in Equation (15).

Different elimination operations are employed in different phases. Strategy 1 generates filling individuals based on the

1) PSO_Prey behavior:

$$X_{1/next} = \begin{cases} X_1 + c_1 \times Randn \times Step \times \dfrac{X_2 - X_1}{\|X_2 - X_1\|} + F \times c_2 \times Randn \times (gbest - X_1), Y_1 < Y_2 \\ X_1 + c_1 \times Randn \times RandStep + F \times c_2 \times Randn \times (gbest - X_1), Y_1 \ge Y_2 \end{cases} \tag{9}$$

2) PSO_Swarm behavior:

$$X_{i/next} = \begin{cases} X_i + c_1 \times Randn \times Step \times \dfrac{X_c - X_i}{\|X_c - X_i\|} + F \times c_2 \times Randn \times (gbest - X_i), \\ Y_c/n_f > \delta Y_i \\ PSO\_\Pr ey(X_i), Y_c/n_f \le \delta Y_i \end{cases} \tag{10}$$

3) PSO_Follow behavior:

$$X_{i/next} = \begin{cases} X_i + c_1 \times Randn \times Step \times \dfrac{X_{\max} - X_i}{\|X_{\max} - X_i\|} + F \times c_2 \times Randn \times (gbest - X_i), \\ Y_{\max}/n_f > \delta Y_i \\ PSO\_\Pr ey(X_i), Y_{\max}/n_f \le \delta Y_i \end{cases} \tag{11}$$

4) PSO_Random behavior:

$$X_{i/next} = X_i + c_1 \times Randn \times RandStep + F \times c_2 \times Randn \times (gbest - X_i) \tag{12}$$

5) PSO Global Guidance Behavior:

$$\begin{cases} W = W_{\max} - (W_{\max} - W_{\min}) \times \dfrac{t}{T} \\ X_{i/next} = X_i + W \times Randn \times Step \times (pbest - X_i) + F \times c_2 \times Randn \times (Tag - X_i) \end{cases} \tag{13}$$

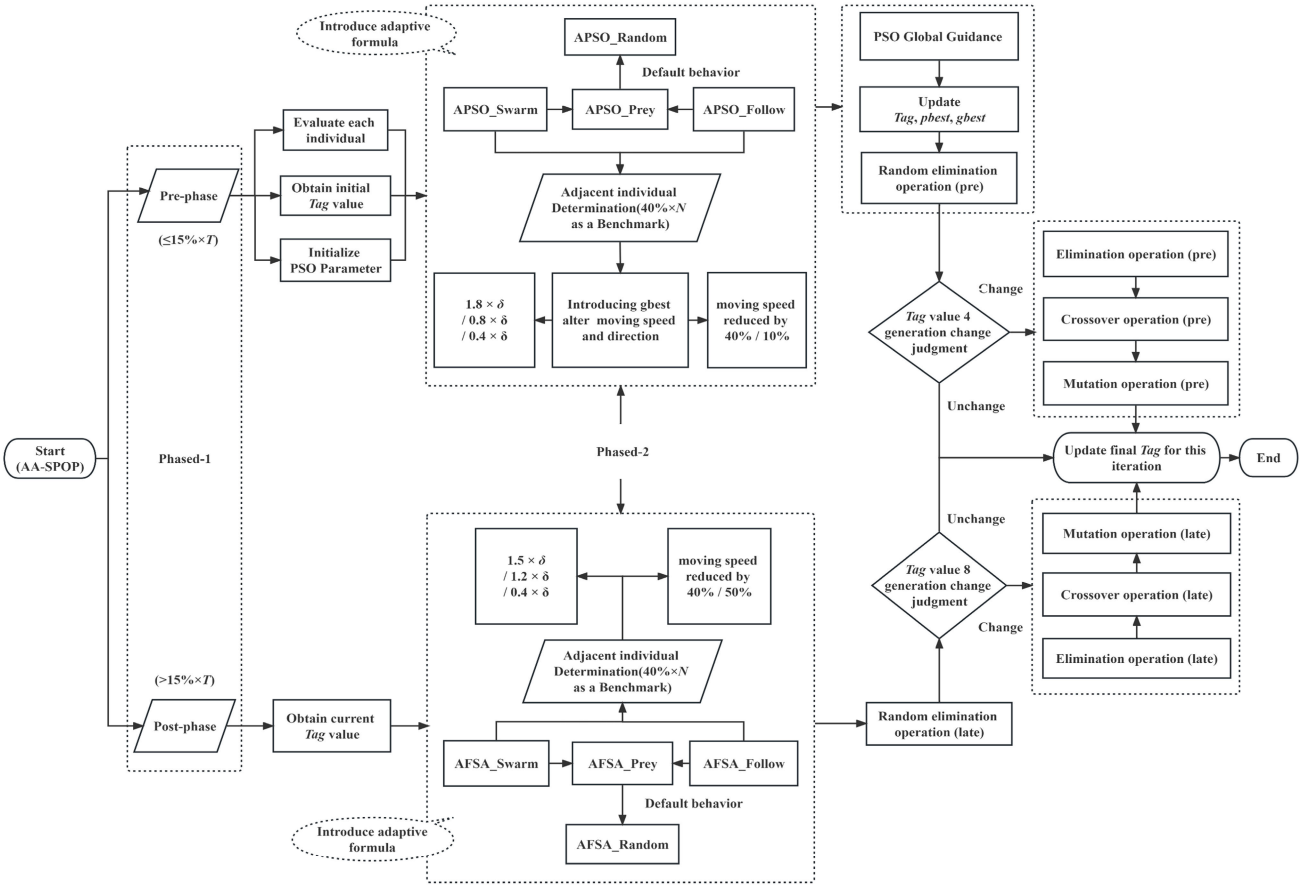

FIGURE 8. Flowchart of the AA-SPOP algorithm.

best fitness value, ensuring algorithm stability and accelerating convergence speed. Strategy 2 increases the mutation rate to introduce more randomness, aiming to escape local optima. In Strategy 1, X_{best1}, X_{best2}, and X_{best3} represent the information of the top three path individuals in the population, ordered by their fitness values $Y_{best1} > Y_{best2} > Y_{best3}$, where $n1$ and $n2$ represent mutation parameters. In Strategy 2, the function *mutation* is used to implement mutation elimination. X_{fill} represents randomly selected individuals from the remaining population after elimination, which are used for filling. *pmutation* represents the mutation rate, *sigma* represents the Gaussian variable, *s* represents the Gaussian parameter, and *bound* represents the range of values for individuals.

b: CROSSOVER AND MUTATION ADJUSTMENT OPERATION

The crossover and mutation adjustment operations are widely applied in the early and late phases of algorithm iteration, triggered based on predefined thresholds. These operations are activated when the *Tag* remains unchanged for a consecutive duration, aiming to break free from local optima. After experimental analysis, to enhance the precision and robustness, and adaptability of the algorithm, the threshold for determining the early and late stages was set at 4 iterations and 8 iterations, respectively. The following provides a detailed description:

$$X_{new} = cross\,(X_{best}, X_{best1}, pcross) \tag{16a}$$
$$0.6 \le pcross \le 0.9 \tag{16b}$$
$$2 \le num\_cross \le 5 \tag{16c}$$

For the crossover adjustment operation, a tournament method is used to select the best individuals for crossover, and a single-point crossover is applied based on the Equation (16). *cross* represents the function for performing crossover operations, with parameters including the best individuals of the entire population (X_{best}), the best individuals selected by the tournament method (X_{best1}), and the crossover rate (*pcross*). The parameter *num_cross* denotes the number of individuals involved in the crossover operation. In the early phase, in order to accelerate convergence speed, the parameter *pcross* is increased and the parameter *num_cross* is decreased. In the late phase, to ensure algorithm stability and accuracy, the parameter *pcross* is reduced and the parameter

num_cross is increased.

$$X_{new} = mutation\,(X_m, pmutation, sigma) \tag{17a}$$
$$sigma = m \times (bound_{\max} - bound_{\min}) \tag{17b}$$
$$0.1 \le pmutation \le 0.25 \tag{17c}$$
$$2 \le num\_mutation \le 8 \tag{17d}$$

For the mutation adjustment operation, Gaussian mutation is applied in both the early and later phases of iteration. It involves selecting relatively superior individuals using the tournament method and is based on the Equation (17). *mutation* represents the function that implements the mutation operation. It takes several parameters, including the best-mutated individual selected through tournament method selection (X_m), the mutation rate (*pmutation*), and the Gaussian variable (*sigma*). Here, *m* represents the Gaussian parameter, and *num_mutation* denotes the number of individuals undergoing the mutation operation. In contrast to elimination mutation, both the individuals and mutation rate differ, and both *sigma* and *pmutation* should be reduced. Additionally, similar to the crossover operation, the values of *pmutation*, *sigma*, and *num_mutation* are smaller in the early phase compared to the later phase

IV. PIPE COLLABORATIVE LAYOUT METHOD

The layout of ship piping systems primarily involves coordinating multiple pipes and their arrangement with other equipment and structures. Current research predominantly focuses on layout for individual pipe, with limited consideration for their collaborative. This paper introduces three novel methods for the collaborative arrangement of the entire piping system, as detailed below:

A. OPTIMIZATION METHOD FOR SINGLE PIPE LAYOUT

The optimization of ship pipe layout primarily focuses on the path optimization of single pipes within the entire piping system layout. It demands a high level of precision and stability from the optimization algorithm, as the layout significantly impacts the overall effectiveness of the piping system. The workflow for single-pipe layout is illustrated in Fig. 10, with the primary generation principles for pipe paths referencing Fig. 3. Each path is formed by connecting coordinate vector points, optimizing the path based on objectives and constraints. This layout method initially involves determining the relative positions of the starting and ending interface points to establish the number of coordinate vector points (path elbows). It primarily falls into three main scenarios, as illustrated in Table 2.

As shown in Table 2 and Fig. 9, within the three-dimensional cabin space, the positions of the start and end points can be categorized into three main scenarios based on coordinate analysis: collinear, coplanar, and non-coplanar. Each of these scenarios corresponds to different requirements for coordinate vector points. According to real-time inquiries from naval engineers, in actual engineering design, the number of pipe elbows (coordinate vector points) is generally no more than three [34], and fewer elbows are preferred. Therefore, the algorithm sets different initial coding vector quantities corresponding to different situations, aiming to achieve targeted optimization. Building upon the aforementioned initialization process, the optimized single-pipe layout method is further implemented, as illustrated in Fig. 10. *Tag*, *t* and *T* have been previously explained. *ct* is the optimum value calculator to determine if the algorithm is trapped in a local optimum, while *BestIndex* represents the best path information. The process primarily comprises three stages as follows:

TABLE 2. Initial conditions of single pipe routing.

Situation	Point coordinate	Elbow number	Code vector
collinear	$\begin{cases} x_1 \neq x_2 \\ y_1 = y_2 \\ z_1 = z_2 \end{cases}$	≤ 1	(x_1, y_1, z_1)
coplanar	$\begin{cases} x_1 \neq x_2 \\ y_1 \neq y_2 \\ z_1 = z_2 \end{cases}$	≤ 2	$\begin{pmatrix} x_1, y_1, z_1 \\ x_2, y_2, z_2 \end{pmatrix}$
non-coplanar	$\begin{cases} x_1 \neq x_2 \\ y_1 \neq y_2 \\ z_1 \neq z_2 \end{cases}$	≤ 3	$\begin{pmatrix} x_1, y_1, z_1 \\ x_2, y_2, z_2 \\ x_3, y_3, z_3 \end{pmatrix}$

1) The first phase is the foundation of the single pipe layout, which involves the initialization of the algorithm. This phase includes the generation of the initial population, determination of the number of coordinate vector points, setting layout space parameters, and configuring various algorithmic parameters, and so on.

2) The second phase primarily involves the crucial determination and constraints of the single-pipe layout. This includes assessing the number of iterations, dividing the pre- and post-iteration phases, and triggering the decision for cross-mutation adjustment operations.

3) The third phase focuses on the algorithm's core execution for the single-pipe layout, which means the implementation of the AA-SPOP algorithm logic. Note that the *ct* and *Tag*, *BestIndex* are updated after the algorithm execution is completed, and finally the optimal path information is obtained.

B. OPTIMIZATION METHOD FOR BRANCH PIPE COLLABORATIVE LAYOUT

Branch pipes account for more than half of the entire ship's piping system design, and it directly impacts the operational efficiency of various systems within the engine room. As shown in Fig. 11 (a), each branch pipe has a starting point (S) and multiple branch endpoints (T). These branching points are typically selected from the main pipe path, which is usually predetermined by engineers or chosen based on criteria such as maximum diameter and maximum distance (As illustrated by side pipe1 in the figure). The collaborative

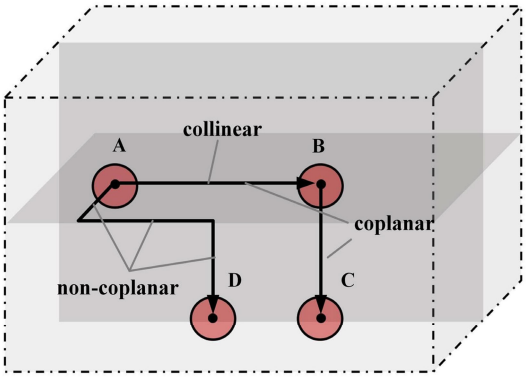

FIGURE 9. The example of single pipe routing.

arrangement of branch pipes requires considerations of branch point locations, individual path characteristics, and overall overlapping degree [20]. It is advisable to prioritize the placement of main conduits when designing branch pipes [35]. Currently, many commonly applied approaches treat the branch pipe problem as a ''one-to-many'' problem, where multiple individual pipes guide each other for placement. However, this approach exhibits poor stability and is susceptible to mutual interference and other issues. Fig. 11(b) and (c) illustrate typical layout problems stemming from this approach. Fig. 11(b) emphasizes the layout of each single pipe to an extent that compromises overall collaborative. In contrast, Fig. 11(c) overly prioritizes overall overlap. This paper introduces a novel approach to collaborative branch pipe layout. This method aims to significantly enhance the efficiency of branch pipe layout, ultimately achieving the ideal collaborative layout depicted in Fig. 11(c).

1) SELECTION METHOD OF VECTOR PROJECTION FOR BRANCHING POINTS

In the layout of branch pipes, the fitness function formula takes into account the calculation of branching points (similar to the starting points of single pipes), resulting in a change in the dimensionality of the vectors. The mathematical expression of multidimensional vectors for branch pipes and the evaluation objective function are shown in Equation (18). In this equation, B represents the branching point, initially located on the main pipe path for ease of optimization, later to be decomposed into three-dimensional coordinate points. n_0- n_m are weight parameters, and the evaluation function for branch pipes consists of evaluation criteria for the main pipe as well as each branch side pipe. At this point, the number of coordinate vector points also becomes the sum of coordinate vector points for the main pipe and branch side pipes.

$$P = \{B, x_1, y_1, z_1, f_1, l_1, \cdots, x_n, y_n, z_n, f_n, l_n, E\} \tag{18a}$$

$$F_{branch} = n_0 \times F_{main} + (n_1 \times F_1 + \cdots + n_m \times F_m) \tag{18b}$$

Finding branching points is of paramount importance in ship branch pipe layout. To address current challenges, this

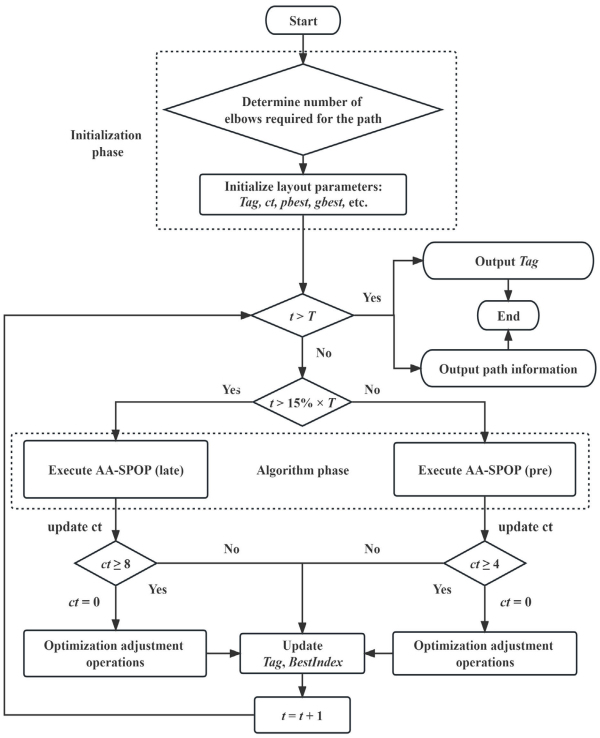

FIGURE 10. Single-pipe layout optimization process.

paper introduces the Branch Vector Projection Optimization Rule. It considers multiple scenarios for locating branching points to achieve the optimal layout for branch pipes, as depicted in Fig. 13. The specific steps of this method are detailed as follows:

Step 1: Using vector projection, identify the initial optimal branching point on the main pipe path. Fig. 12 and Algorithm 1 illustrate this method. Each branching point projects vectors onto segments of the main pipe and already placed pipes to determine the locations of their orthogonal points. Fig. 13 shows a layout model with three branching points, P1, P2, and P3. By calculating vector ratios for each segment of the main pipe (in black) and existing pipes (in yellow), it's determined whether intersection points exist within the path. Ultimately, P1 obtains orthogonal projection points T1, T2, and T3, P2 obtains points T5 and T3, while P3 lacks any projection points along the path.

Step 2: Assess the presence of obstructions between projections and use the square-crossing method to add extension points. The principle of this method is illustrated in Fig. 14, where a virtual square frame is created with two points as diagonals to detect obstruction scenarios, thereby determining the need for extension points. As shown in the Fig. 14, there are no obstructions between the two squares at branching endpoint P1. However, obstructions are present between the squares at branching endpoint P2. Consequently, extension points are selected along the edges of the obstructions between the squares to bypass obstacles. This process

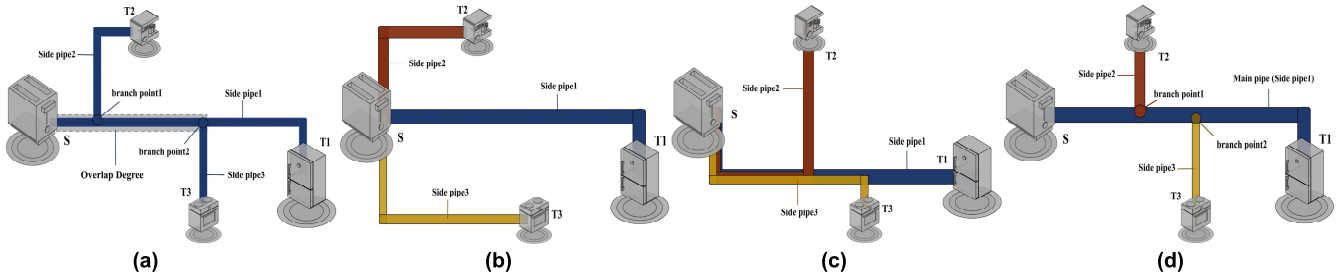

FIGURE 11. Principles analysis of collaborative layout for branch pipes. (a) Schematic diagram of branch pipes principle. (b) Layout result 1 with traditional methods. (c) Layout result 2 with traditional methods. (d) Ideal layout result.

Algorithm 1 Vector Projection Function

Input: Line_segment (Main pipe segmented path)
Point (Branch endpoint)
Output: Intersection_ p (Initial optimal branch point)

$P1\ (x_1, y_1, z_1)$, $P2\ (x_2, y_2, z_2) \leftarrow$ line_segment
$(p\_x, p\_y, p\_z) \leftarrow$ Point
Compute the direction vector of the segmented path
$l\_v = (x_2 - x_1, y_2 - y_1, z_2 - z_1)$
Calculate vector $PP1$
$PP1 \leftarrow$ (Point, $P1$)
$PP1 \leftarrow p\_x - x_1, p\_y - y_1, p\_z - z_1$
Calculate projection parameter T
$T \leftarrow Num/Den \leftarrow dot(PP1, D)/dot(D, D)$
$Num = PP1[0] \times l\_v[0] + PP1[1] \times l\_v[1] + PP1[2] \times l\_v[2]$
$Den = l\_v[0] \times l\_v[0] + l\_v[1] \times l\_v[1] + l\_v[2] \times l\_v[2]$
Check for intersection between the point and the path
if ($Den == 0$):
  Return None
elif ($Num! = 0$ and $0 \leq T \leq 1$):
  Calculate the coordinates of the intersection point intersection_p (x_t, y_t, z_t)
  $x_t \leftarrow x_1 + T \times l\_v[0]$
  $y_t \leftarrow y_1 + T \times l\_v[1]$
  $z_t \leftarrow z_1 + T \times l\_v[2]$
  Return intersection_p
else:
  Return None
end if

ultimately yields extension points T4, T6, T7, T8, and T9 (as depicted in Fig 14).

Step 3: After calculating the projection and extension points for each branching endpoint, to prevent situations where no suitable branching point is available (e.g., branching endpoint P3 in Fig. 13), consider the existing pipe elbows as potential branching points. Specifically, select the nearest elbow point as the branching point based on the principle of proximity (e.g., point c3 in Fig. 13).

$$W\_Value = v_1 \times Distance\_v + v_2 \times Obstacle\_v + v_3 \times Power\_v + v_4 \times Elbow\_v \quad (19a)$$

$$Distance\_v = |x_i - x_{i+1}| + |y_i - y_{i+1}| + |z_i - z_{i+1}| \quad (19b)$$

$$Obstacle\_v = o_1 \times num\_obs + o_2 \times s\_edge \quad (19c)$$

$$Power\_v = w_1 \times overlap\_part \quad (19d)$$

$$Elbow\_v = b_1 \times num\_obs \quad (19e)$$

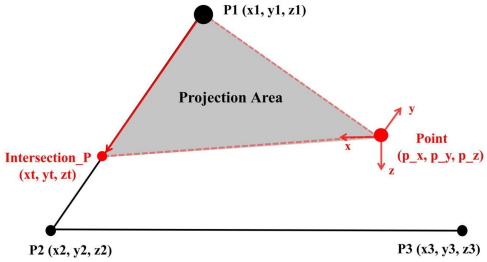

FIGURE 12. Vector projection method example.

Step 4: Evaluate the optimal branching point. Through calculations involving projection intersection points, extension points, and elbow points, a list containing all potential branching points is generated. To assess the quality of each point, a branching point evaluation formula, as shown in Equation (19), is designed, taking into account factors such as distance, the number of elbows, energy zones, and obstruction indicators. In Equation (19), *Distance_v* evaluates the distance value, *Obstacle_v* evaluates the obstruction situation in the square crossing lines, *num_obs* evaluates the number of obstructing obstacles, *s_edge* evaluates the shortest edge length of the obstacles, v_1-v_4, o_1, o_2, w_1, and b_1 are the corresponding weighting parameters. *Power_v* evaluates the degree of passage through an energy zone, and *Elbow_v* evaluates the number of elbow points considering the obstruction range of obstacles.

Step 5: Obtain the Optimal Branching Point. Following the branch optimization method described above, the selected optimal points are T2, T7, and c3. One of the resulting best layout configurations is illustrated in Fig. 15 below, representing the optimal path.

2) COLLABORATIVE LAYOUT PROCESS OF BRANCH PIPES

The concept of cooperative evolution is generally aimed at achieving multiple mutually beneficial objectives. After

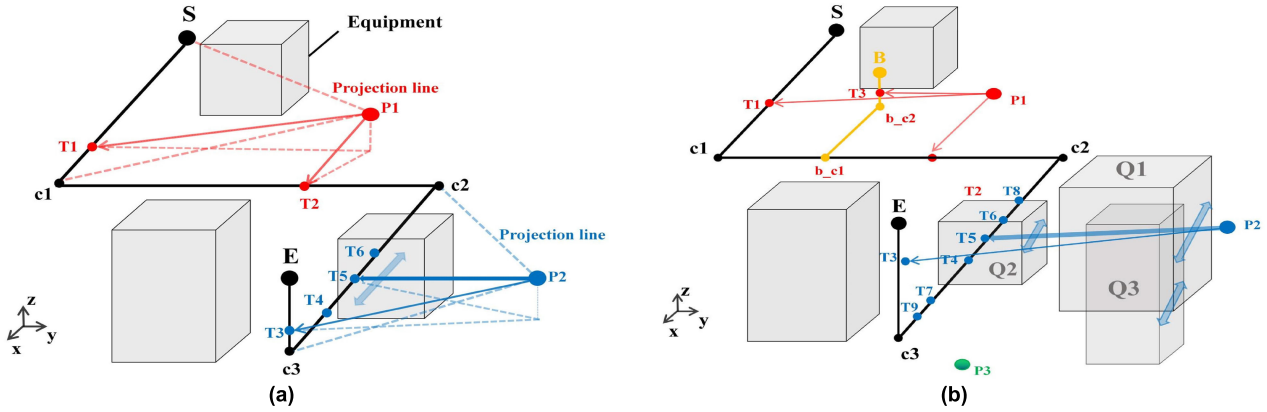

FIGURE 13. The example for selecting the vector projection of branch points. (a) Simple projection layout. (b) Complex projection layout.

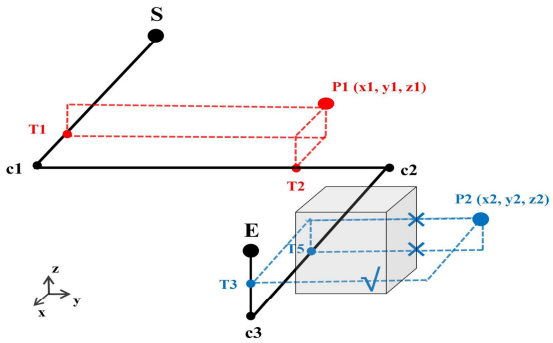

FIGURE 14. The example of square crossing for determining expansion points.

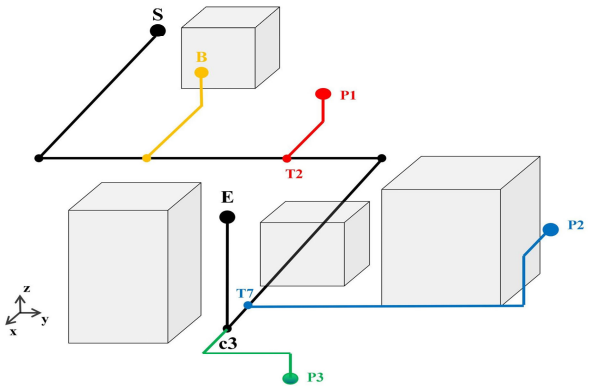

FIGURE 15. One of the optimal collaborative layout schemes.

the crucial step of branch point identification, the algorithm presented in this paper integrates the principles of cooperative evolution [29] to propose a branch pipe layout method (Fig. 16). The specific steps are as follows:

Step 1: Initialization. Initialize the initial population of the main and branch pipes, layout parameters, algorithm parameters, and the initial required vector connection points for each pipe.

Step 2: Check if the iteration count t meets the stopping criteria. If it does, output the optimal fitness value *Whole_Tag* and obtain the optimal path information for the entire pipe. Otherwise, proceed to Step 3.

Step 3: Execute the operations corresponding to the early and late stages of the AA-SPOP algorithm based on the current iteration phase (as shown in Fig. 8).

Step 4: Determine the positions and optimization sequence of the main and branch pipes. Start by laying out the main pipe, and once the main pipe path is established, the placement order of branch pipes is determined based on the principle of prioritizing shorter distances between the main pipe's start and end points and the branch endpoints. Update the *Tag*, path, energy zone, and obstacle information promptly after each pipe is laid out.

Step 5: Sequentially optimize each branch pipe. Begin by determining the coordinates of the branch starting point C using the branch point optimization method based on the *main_path*. Then, execute the algorithmic operations. After completing the layout of each branch pipe, update *siden_Tag*, *siden_path*, obstacle, and energy zone information. The completed branch pipes are designated as obstacles (to prevent subsequent pipes from crossing) and surrounded by an additional energy zone layer. This is primarily to guide the layout of subsequent pipes.

$$Whole\_Tag = w_0 \times mian\_Tag + w_1 \times side1\_Tag + \cdots + w_n \times siden\_Tag \tag{20}$$

Step 6: After completing optimization for all pipes in this iteration, the overall optimal fitness value *Whole_Tag* and optimal path information are updated according to Equation (20), where *main_Tag* and *siden_Tag* represent the optimal fitness values for the main pipe and branch pipes, respectively. By adjusting the weight parameters w_1-w_n for each pipe, the layout priority and importance of each pipe can be controlled.

Step 7: The obstacles and energy zone information is reset to its initial state. Execute the next iteration, make $t = t + 1$ and return to Step 2.

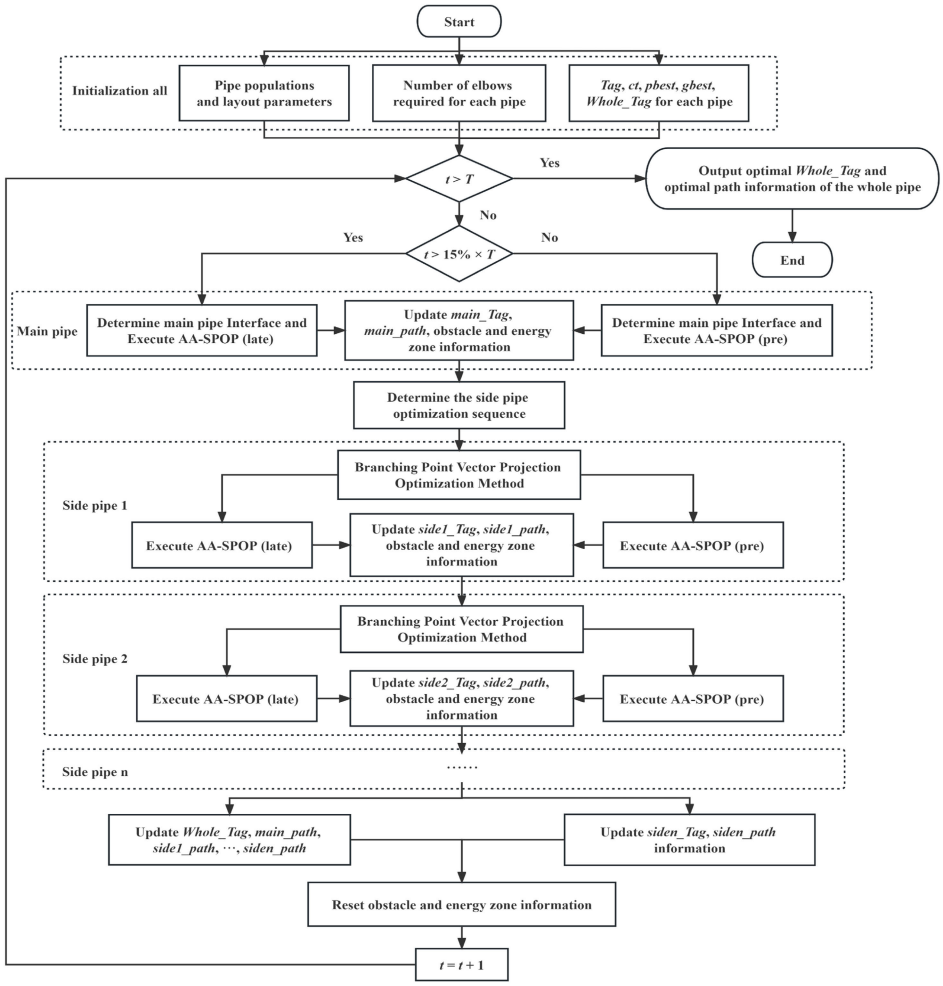

FIGURE 16. Process of the collaborative layout optimization method for branch pipes.

C. OPTIMIZATION METHOD FOR PIPE AND SUPPORT EQUIPMENT COLLABORATIVE LAYOUT

Currently, research on the SPRD problem predominantly focuses on pipe layout, with insufficient consideration for other factors within the cabin. Achieving collaborative between pipes and equipment is a critical challenge that needs to be addressed. pipe and equipment collaborative optimization refers to the optimization of the layout of pipes and support equipment (including fixed pipe clamps and hangers) to ensure ship safety, pipe system efficiency, and stability. According to regulatory requirements, support equipment should be installed based on the pipe system's needs for clamps, brackets, overall layout requirements, and the ship's structural design. Moreover, it must be installed on reliable structures, with efforts made to maintain parallel alignment between supports and the pipe system [36]. The primary function is to withstand pipe pressure and displacement.

This paper, based on engineering practical cases and design standards, presents an energy-based guiding collaborative layout method as follows:

Step 1: Initialize parameters for each component.

Step 2: Check if iteration count t satisfies the termina-tion criteria. If it does, output the optimal *Tag*, the overall optimal path information, and equipment positions. Otherwise, proceed to Step 3.

Step 3: Definition of the energy guidance range in cabin spaces. The arrangement of support equipment should be based on the ship's cabin structure and operational requirements. Prior to the layout of pipes, it is necessary to initialize and determine the initial requirements and quantities of support equipment for each pipe, establish an appropriate range for the placement of support equipment, and delineate the energy-guided area. As shown in Fig. 17(a), the shaded area represents the energy-guided region, with varying degrees of guidance in different areas. It primarily signifies suitable installation zones, providing guidance for pipe layout. The energy values can be adjusted according to specific requirements.

Step 4: Determination of the energy guidance range along the pipe path. To achieve optimal collaborative in both

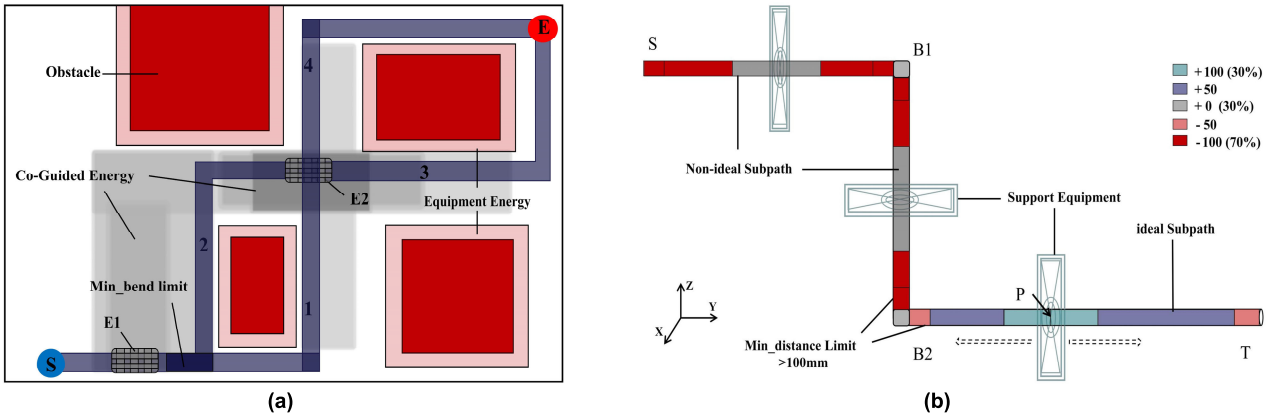

FIGURE 17. Principle of collaborative layout of pipe and equipment. (a) Energy guidance principles for equipment. (b) Energy guidance principles for pipes.

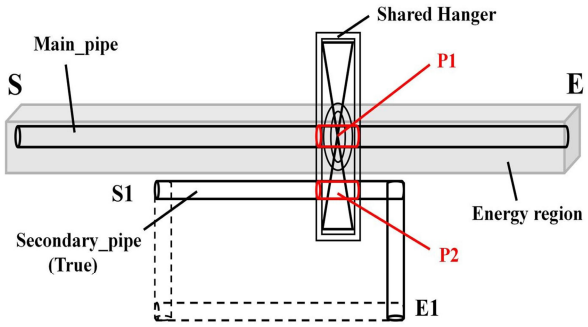

FIGURE 18. Pipe and equipment collaborative layout example.

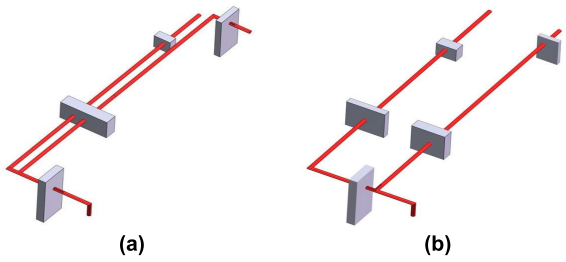

FIGURE 19. Support equipment layout. (a) Shared support bracket scenario. (b) Non-shared support bracket scenario.

aspects, the pipes themselves have corresponding energy zones. In practical engineering, the best layout range is typically defined based on factors such as cargo properties, path length, and stress [37], [38], [39]. In this paper, we prioritize length and divide different layout ranges based on the selection of ideal sub-paths. Each range corresponds to a different energy value, and during each iteration, a random position is selected and evaluated to choose the optimal location. As shown in Fig. 17(b), the selected ideal sub-path is between B2 and T, where different levels of positive energy values guide the layout. The remaining two segments represent non-ideal layout sub-paths, assigned negative energy values to repel them. Additionally, compliance with the requirement of a minimum bending distance of no less than 100 mm is considered in accordance with regulations.

Step 5: Commence the Collaborative Layout Process.

1) First, determine the layout priority and the required number of suitable support equipment for each pipe based on the diameter and engineering requirements. Then, divide the energy guidance areas for both aspects.

2) Continuously update the energy and obstruction areas after completing the layout for each pipe to facilitate the layout of the remaining pipes. For instance, in Fig. 18, the secondary pipe should be placed close to the main pipe layout to allow for the generation of shared hanger and compliance with parallelism requirements. Note that support points p1 and p2 should be spaced less than 300mm apart to meet the requirements of shared structure. Additionally, in practical pipe layouts, different layouts are implemented based on engineering requirements. Fig. 19 illustrates the actual layout scenarios after envelope processing. Fig. 19(a) represents a situation with shared supports but an increase in elbows, while Fig. 19(b) depicts a scenario with no shared supports but a reduction in elbows and path length. This algorithm can achieve both solutions by balancing the weight values of each objective.

$$\begin{aligned} F_{\max}(path(v)) = W - (&p1 \times Orth(v) + p2 \times Obs(v) + p3 \\ &\times Lenth(v) + p4 \times Elbow(v) \\ &- p5 \times Power(v) - p6 \times F\_L(v) \\ &- P7 \times Bracket(v)) \end{aligned} \tag{21a}$$

$$s.t.g(p) = 0, h(p) = 0, v \in bound \tag{21b}$$

3) Commence the iterative process of the algorithm. It's important to note that the evaluation function for the collaborative layout of pipes and equipment has some variations, as indicated in Equation (21). $Bracket(v)$ represents the energy value of the equipment, denoting the degree of collaboration between the path and the support equipment. $Bracket(v) = \sum_i^N BR(v_i, v_{i+1}, bralist)$, The weight parameter for Bracket(v) is denoted as $p7$. In the model

depicted in Fig. 17(a), it's assumed that two support equipments to be arranged initially on different paths. Based on the energy guidance method described above and the optimization of the algorithm, an ideal result can be achieved: the equipment positions are located in the region with the highest level of gray shading. Additionally, four optimal paths are obtained, namely 1-3, 2-3, 1-4, and 2-4.

Step 6: After completing the optimization of all pipes and support equipment, output the evaluation value *Whole_Tag* for the optimal collaborative layout of pipes and support equipment, along with the corresponding scheme information. Engineers can further adjust the layout based on their specific requirements.

Step 7: Reset obstacle and energy zone information to their initial states. Execute the next iteration, make $t = t + 1$ and return to Step 2.

V. SIMULATION VALIDATION AND ANALYSIS

A. CASE 1: VALIDATION OF ENCODING TECHNOLOGY AND ALGORITHM PERFORMANCE

To validate the efficiency and adaptability of the proposed vector-based encoding scheme and AA-SPOP algorithm in pipe layout applications, this section adopts the layout model from reference [40]. Under the same pipe layout problem and environmental conditions as detailed in the reference, we conduct comparisons with six different types of algorithms from the literature and the previous AFSA algorithm, including comparisons with various encoding methods. The primary objective of this layout model is to evaluate the performance of algorithms in the context of single-pipe layout problems. The tested algorithms from the literature include GA, PSO, FA (Firefly Algorithm), DE, CS (Cuckoo Search) and DDCES (collaborative Differential Cuckoo Search). To ensure the fairness of the comparative tests, this paper maintains consistency with the literature regarding the layout environment, algorithm parameters, and other layout conditions. Some of the algorithms employ a grid-based encoding method (indicated with a "G" suffix), with grid partitioning precision based on pipe diameter.

The layout model for this case, as shown in Fig. 20, is a cubic space with diagonal vertex coordinates at (0, 0, 0) and (50, 50, 50). It's worth noting that the space simulates various types of ship cabin spaces for different scenarios. Within this space, there are 7 obstacles (representing ship equipment) in the form of envelope bodies, with their diagonal vertices located at the following coordinates: $[\{(21, 0, 0), (30, 5, 4)\}_{O1}, \{(6, 0, 0), (16, 5, 50)\}_{O2}, \{(42, 10, 0), (50, 18, 12)\}_{O3}, \{(20, 42, 0), (30, 50, 50)\}_{O4}, \{(42, 26, 0), (50, 42, 12)\}_{O5}, \{(0, 15, 0), (9, 32, 20)\}_{O6}, \{(14, 14, 0), (34, 35, 21)\}_{O7}]$. The coordinates of the starting interface and target interface for the single-pipe design to be optimized are (0, 0, 0) and (50, 50, 50), respectively.

In Case 1, the parameters for the evaluation function of the pipe layout are uniformly set as follows: W: 100; The weighting parameters $p1$ to $p6$ are set in the following proportions: 1: 1: 0.001: 0.001: 0: 0.001. The detailed parameter settings

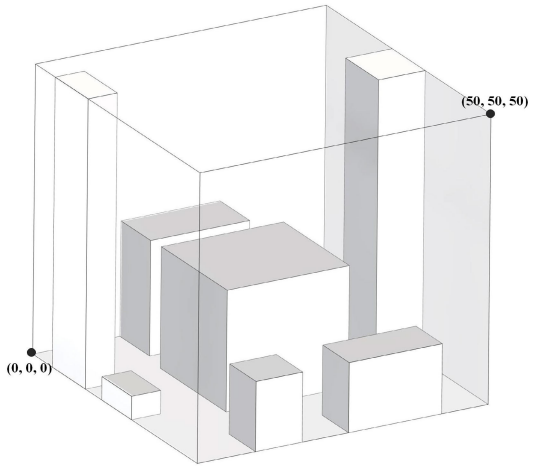

FIGURE 20. Layout space of Case 1.

TABLE 3. Parameter settings for the 8 algorithms in Case 1.

Algorithm	Parameter settings
GA	Vector size: 24, crossover: 0.8, mutation rate: 0.1
PSO	V_{max}: 5, c_1: 2.5, c_2:0.5, W_{ini}: 0.9, W_{end}: 0.4
FA	α: 0.5, β: 0.2, γ: 1
DE	F: 0.5, CR: 0.8
CS	Step: 1, Pa: 0.25
DDCES	Consistent with those in DE and CS
AFSA	Visual:0.04, Step:0.03, δ:0.02, Try_number: 50
AA-SPOP	Consistent with those in AFSA

for each algorithm are shown in Table 3, with the parameters of the original AFSA algorithm kept consistent with the AA-SPOP algorithm. Through verification and analysis of the literature algorithms, these parameters setting primarily based on the magnitude of population changes or step lengths during each iteration operation, which can be calculated based on the algorithm's operation formulas. Parameters are a significant component of these formulas (in the pipe layout problem, a change of around 10% of the maximum model space edge length is optimal), and under these parameters, they all remained in their optimal state. In addition, the initial population size is set to 50. The Case 1 were conducted on a Windows 11 operating system using Python 3.9, running on a 12th Gen Intel(R) Core (TM) i7-12700H processor.

After conducting 30 individual tests for each of the 8 algorithms, the final test results are compared, as shown in Fig. 21 and Table 4. Upon observation, it is evident that, firstly, my computational results are in close agreement with those in the literature (with minor differences due to variations in equipment and methodologies), which adds credibility to this experimental outcome. Secondly, algorithms based on vector encoding perform significantly better than grid-based

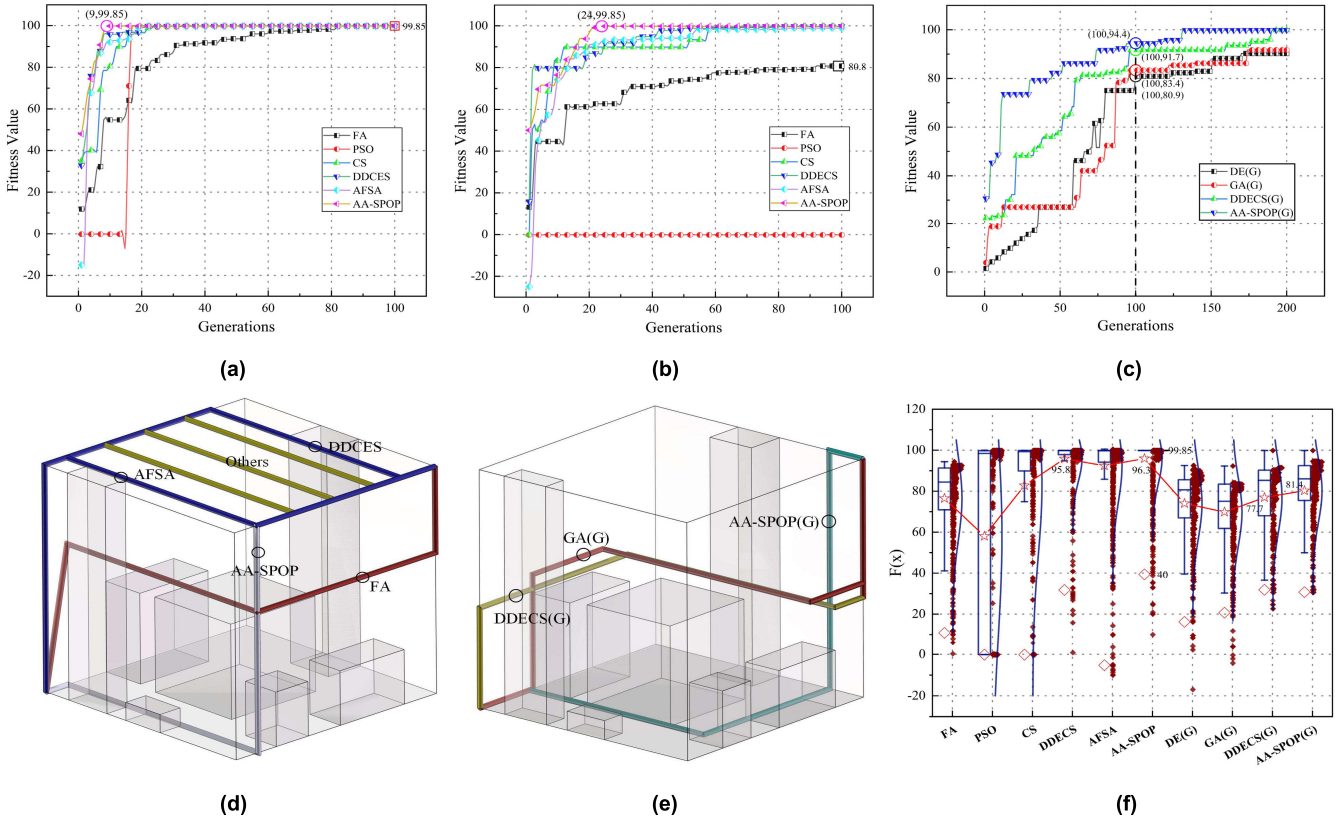

FIGURE 21. Performance comparison of the 8 algorithms. (a) The best results (vector encoding). (b) The worst results (vector encoding). (c) The best results (grid encoding). (d) Optimal layout for each algorithm (vector encoding). (e) Optimal layout for each algorithm (grid encoding) (f) Calculation results for each algorithm consist of 30 sets of tests.

approaches. Among the four grid-based encoding algorithms, they exhibit strong stability but suffer from slow convergence, extended computation time, and reduced precision. Among the six vector encoding algorithms, FA and CS exhibit higher computational accuracy but poorer stability (large standard deviation). The PSO algorithm shows good performance with random initial solutions but lacks stability and is prone to local optima. The hybrid algorithms DDCES and AFSA perform well in all aspects, but their convergence efficiency can be further improved.

In comparison, the AA-SPOP algorithm demonstrates strong characteristics in terms of computational accuracy, stability, robustness and efficiency. In all cases, it consistently obtained the global optimal solution and converged within approximately 20 generations. Fig. 21(d) illustrates the optimization performance of different algorithms for pipe layout when the weight parameter p5 for the energy zone is increased to 0.001 (with energy zones distributed around the equipment and on the surface of the six faces). The pipe layout based on the AA-SPOP algorithm closely aligns with the energy zone, while maintaining minimal elbow count and path length. Fig. 21(d) depicts the layout results after 100 iterations using the grid-based encoding algorithm, which exhibits subpar layout effectiveness. In conclusion, the proposed algorithm and encoding approach demonstrate a degree of feasibility.

B. CASE 2: VERIFICATION AND ANALYSIS OF BRANCH PIPE COLLABORATIVE LAYOUT METHOD

Case 1 demonstrated the superiority of the proposed algorithm and the spatial vector encoding method. Case 2 presents a typical model for branch pipe layout space [41] (Applicable to all types of ships), as shown in Fig. 22. The effectiveness of the proposed branch pipe collaborative layout method has been validated through a comparison with the layout methods and algorithm performance described in reference [41]. The layout space of this case study is a cube with dimensions approximately 40 in length, width, and height, consisting of six obstacles (ship equipment) with their respective diagonal vertex coordinates as follows: [{(6, 12, 1), (24, 16, 40)}$_{O1}$, {(32, 12, 1), (40, 16, 40)}$_{O2}$, {(1, 26, 1), (8, 30, 40)}$_{O3}$, {(16, 26, 1), (34, 30, 40)}$_{O4}$, {(1, 1, 12), (24, 40, 16)}$_{O5}$, {(16, 1, 26), (40, 40, 30)}$_{O6}$]. There are four interfaces with the following coordinates in this case: (20, 40, 20), (20, 1, 1), (1, 40, 40), and (40, 20, 30).

The branch pipe layout belongs to the typical one-to-many problem. The approach outlined in reference [41], which is commonly employed, decomposes the branch pipe layout problem into individual pipe optimization problems with different populations and integrates the ecological concept of collaborative evolution. In this model, the problem is initialized with a common starting point and three branch endpoints. In contrast, the collaborative layout method

TABLE 4. Comparison of test results for different algorithms in Case 1.

Indicator	GA(G)	DE(G)	DDCES(G)	AA-APOP(G)	FA	PSO	CS	DDCES	AFSA	AA-SPOP
Optimal value	92.27	90.47	99.85	99.85	92.40	99.85	99.85	99.85	99.85	99.85
Average value	87.98	88.91	97.46	98.84	88.28	99.85	99.85	99.85	99.85	99.85
Worst value	78.88	87.16	88.75	90.62	79.39	99.79	99.848	99.85	99.85	99.85
Standard deviation	4.92	1.81	3.23	2.23	4.68	0.03	0.001	0	0	0
Average convergence algebra	300+	300+	200+	200+	100+	51.4	57	33.7	27.6	14.2
Average calculation time/ s	4.2	4.7	20.2	24.5	2.1	40.2	5.2	6.1	5.8	10.1

presented in this paper, as described in Section IV, selects the two interfaces furthest apart as the starting and ending points for the main pipe, which in this case are (20, 1, 1) and (1, 40, 40), while the other two branch endpoints are (40, 20, 30) and (20, 40, 20).

In order to validate the feasibility of co-evolutionary method proposed in this paper, we compared it not only with the methods in the literature but also with the high-performing algorithms (including DDECS and AFSA) and encoding methods used in Case 1. In this context, the suffix "T" in the algorithm names indicates the adoption of traditional methods, while "G" signifies the use of grid-based encoding. The algorithm parameters were kept consistent with those in Case 1, with a limit of 100 iterations. The population size for each pipe is set to 50. Regarding the overall fitness evaluation, the fitness values for the main pipe and side pipes are weighted in a ratio of 0.65:0.35. The value of C for each pipe is 225, and the weighting parameters for the evaluation function, $p1$ to $p6$, are set in the following proportions: 1: 10: 1: 1: 0.01: 0.01. To facilitate better comparison with the literature, the maximization problem is transformed into a minimization problem by adjusting the signs of the final fitness values. Both co-evolutionary methods do not consider the order of branch pipe layout. Each algorithm was run 30 times, and the best layout results were compared, as shown in Fig. 23. Fig. 23 (a) represents the model space after grid-based processing, where the grid precision is based on the pipe diameter. Algorithm performance comparisons are presented in Fig. 24, and the layout results are detailed in Table 5 (layout results limited to 100 iterations).

According to the test results, the co-evolutionary layout method proposed in this paper demonstrates significant advantages across various evaluation criteria. Specifically, in terms of layout methods, there is not a significant difference in algorithm performance, but the pipe co-evolution degree is higher when employing the layout method proposed in this paper, exceeding 20%. In terms of encoding methods, the algorithms using the encoding method proposed in this paper exhibit faster optimization rates and higher precision. These results can be referenced through the testing outcomes of two different encoding methods of the DDECS and AA-SPOP algorithms. In terms of algorithm performance, based on the evaluation criteria, AA-SPOP>DDECS>AFSA, but the AA-SPOP algorithm also has certain drawbacks, as it is relatively less time-efficient compared to the DDECS algorithm. Nevertheless, this time efficiency metric is not highly critical in the context of pipe layout. In conclusion, the co-evolutionary layout method proposed in this paper is highly efficient and practical.

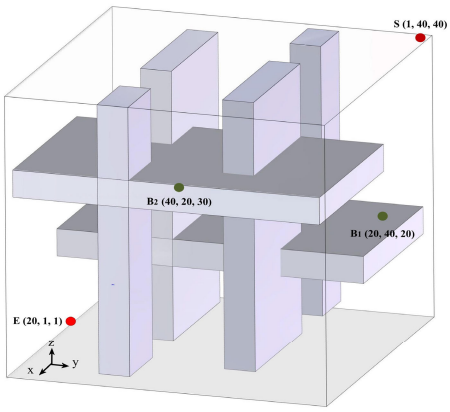

FIGURE 22. Layout space of Case 2.

C. CASE 3: VERIFICATION AND ANALYSIS OF COLLABORATIVE LAYOUT METHOD FOR VARIOUS PIPE AND SUPPORT EQUIPMENT

Cases 1 and 2 have demonstrated the effectiveness of the algorithm, encoding method, and branch collaborative layout method. Case 3 is primarily aimed at verifying the engineering practicality of the proposed AA-SPOP algorithm and the collaborative layout optimization method for mixed pipes and support equipment. It is based on the pipe layout of an actual nuclear-powered ship, representing a complex large-scale layout model compared to the previous two cases, as shown in Fig. 25. The actual layout space has dimensions of 6000mm (length) × 8000mm (width) × 5000mm (height). Fig. 25(a) and Fig. 25(b) present the actual engineering drawings, with annotations for some pipes and support equipment, while Fig. 25(c) shows the processed equipment envelope model. In the figures, represents the pipe label, E represents the

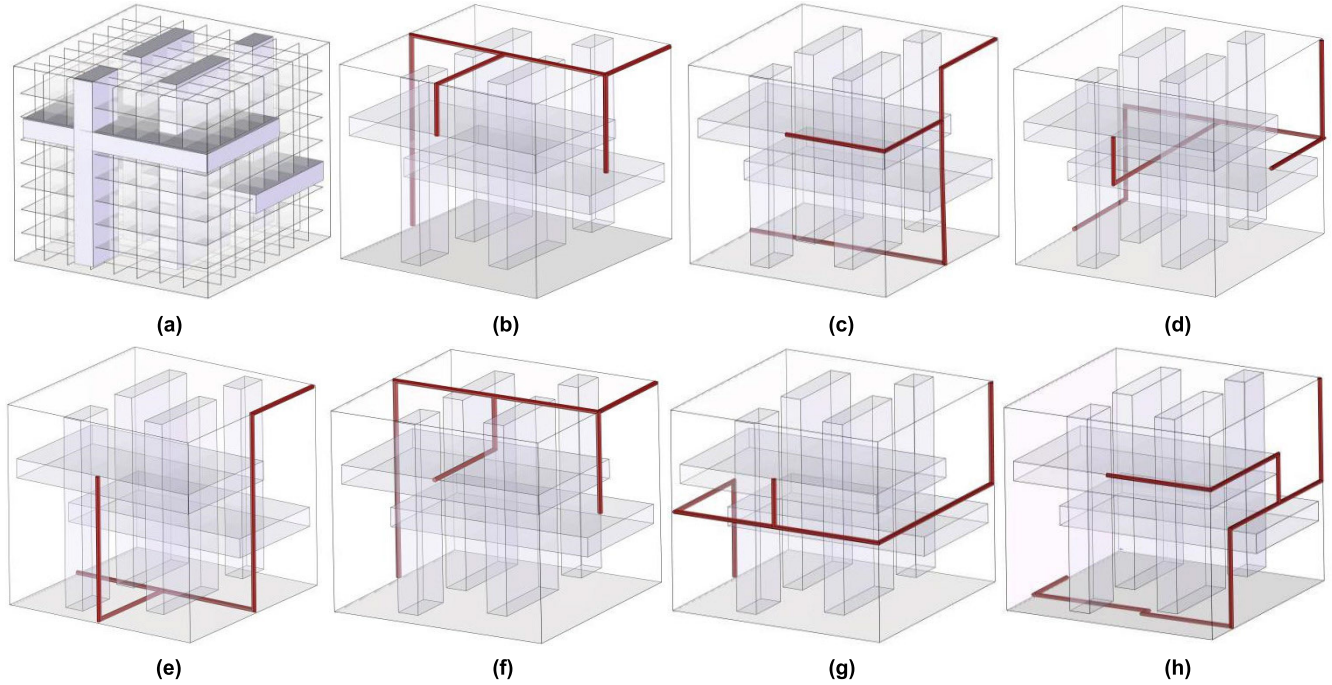

FIGURE 23. Comparison results of the collaborative layout. (a) Grid-based representation. (b) AA-SPOP algorithm. (c) AA-SPOP(T) algorithm. (d) AA-SPOP(G) algorithm. (e) AFSA algorithm. (f) DDECS algorithm. (g) DDECS(G) algorithm. (h) Literature algorithm.

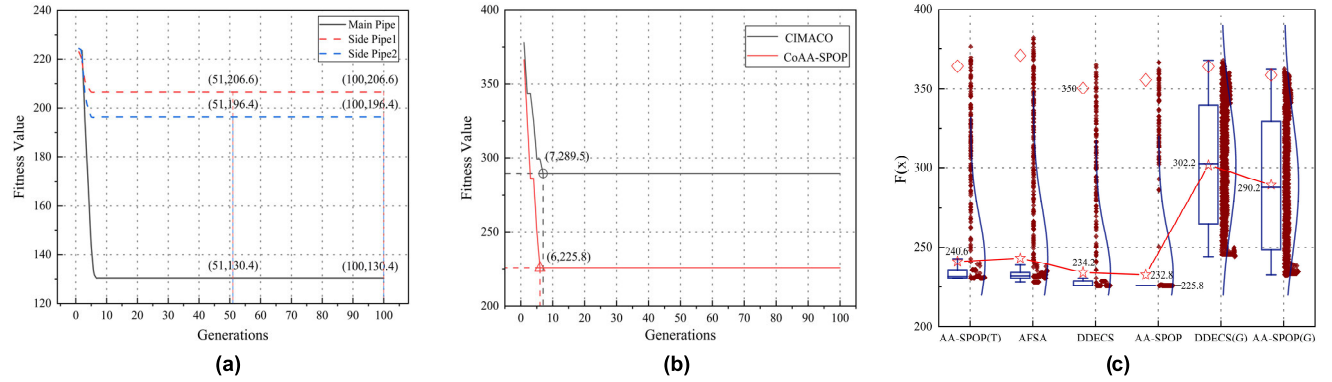

FIGURE 24. Comparison of the performance between these algorithms. (a) The performance of branch pipe in this paper's algorithm. (b) Comparison of the overall performance with literature algorithm. (c) Comparison of the complete test results of the algorithms.

equipment label, and S-E represents the support equipment label. Detailed information on the original layout of each pipe can be found in Table 6. Due to the confidentiality of certain equipment and penetrations involved in pipe connections, detailed disclosure of equipment information is avoided, considering the specific nature of nuclear-powered ship.

In the complex and extensive space of Case 3, to comprehensively validate the effectiveness of our approach, we conducted comparisons not only with the original engineering design but also with the high-performing DDECS algorithm and the AA-SPOP algorithm under grid encoding. The algorithm parameters were set consistent with the previous two cases, with grid partitioning precision based on pipe diameter. Evaluation functions followed Equation (21). The initial C values for both the main pipe and branch pipes are set to 1500 (considering the large layout space). The main-branch ratio for the branch collaborative layout method is set to 0.65:0.35. The weight parameters of the fitness function, $p1$ to $p7$, are set in the following proportions: 1:10:0.001:0.01:0.001:0.1:0.1. The population size is set to 50, and the number of iterations was set to 200. When arranging the pipes, they are sorted based on their diameter, with priority given to pipes with larger diameters.

Case 3 represents a typical large-scale layout scenario found in real nuclear-powered ships. Its primary purpose is to provide a comparative validation of this paper's cooperative layout methodology, encoding approach, algorithm performance, and engineering practicality. The test results

TABLE 5. Comparison of test results for different algorithms in Case 2.

Indicator	CIMACO(T)	AA-SPOP(T)	DDECS(G)	AA-SPOP(G)	DDECS	AFSA	AA-SPOP
Optimal value	289.5	230.8	244.8	232.2	225.8	228.2	225.8
Elbow_num	9	4	5	5	4	4	4
Length	175	147	165	147	147	147	147
convergence algebra	7	9	100+	100+	9	13	6
Overlap degree	0	0.136	0.352	0.272	0.408	0.265	0.408
Average calculation time/ s	-	22.1	62.1	74.4	20.3	18.6	24.7

TABLE 6. Layout information for Case 3.

Pipe ID	Type	Interface Coordinates (mm)	Support Equipment Coordinates (mm)	Connected Equipment information (mm)	Diameter (mm)
P1 P1-1 P1-2	Branch pipe	S1: (74805, -33900, 440) E1: (73286, -29595, 730) E1-1: (73850, -34892, 230) E1-2: (73700, -35300, 650)	S-E 1: (74163, -33900, 543) S-E 2: (73300, -32298, 729) S-E 3: (73230, -30302, 688) S-E 8: (74168, -34245, 165) S-E 9: (73713, -31750, 665) S-E 10: (73872, -29503, 465)	E-A: Min Point: (74805, -34120, 150) E-A: Max Point: (75925, -33680, 590) E-D: Min Point: (74250, -30588, 555) E-D: Max Point: (76438, -28412, 2700)	36.5 36.5 30
P2 P2-1	Branch pipe	S2: (74950, -33900, 590) E2: (73430, -35750, 4162) E2-1: (73430, -35750, 4162)	S-E 4: (74163, -33900, 440) S-E 5: (73225, -35076, 865) S-E 6: (73290, -35753, 1850) S-E 7: (73438, -35800, 3850)	E-A (Same as above)	30 30
P3	Single pipe	S3: (74861, -33900, 210) E3: (74003, -34903, 210)	S-E 11: (73993, -34707, 135)	E-A (Same as above) E-B: Min Point: (73704, -35106, 120) E-B: Max Point: (74100, -34900, 322)	10.5
P4	Single pipe	S4: (73950, -34891, 150) E4: (76837, -32450, 4000)	S-E 12: (73225, -33591, 162) S-E 13: (74950, -32471, 150) S-E 14: (75618, -32609, 2000) S-E 15: (76284, -32592, 3952)	E-B (Same as above)	30
P5	Single pipe	S5: (73850, -35550, 2387) E5: (76821, -35800, 3850)	S-E 16: (75374, -35825, 3835) S-E 17: (76602, -35825, 3794)	E-C: Min Point: (73639, -35682, 1920) E-C: Max Point: (76215, -35425, 2387)	30
P6	Single pipe	S6: (76008, -35550, 2387) E6: (74420, -35800, 4198)	S-E 18: (74773, -35700, 2577) S-E 19: (74229, -35817, 4100)	E-C (Same as above)	30
P7	Single pipe	S7: (74220, -35550, 2387) E7: (74220, -35800, 4198)	S-E 19: (74229, -35817, 4100)	Confidential equipment.	30
P8	Single pipe	S8: (74165, -33550, 1650) E8: (71732, -32500, 4000)	S-E 20: (74710, -33519, 1658) S-E 21: (75658, -33425, 2804) S-E 22: (74704, -32489, 4018)	Confidential equipment.	24
P9 P9-1	Branch pipe	S9: (74265, -33550, 1150) E9: (76400, -30752, 4300) E9-1: (73820, -34131, 600)	S-E 23: (74760, -33519, 1158) S-E 24: (76411, -31224, 4300) S-E 25: (74614, -33465, 585) S-E 26: (73789, -33700, 413)	Confidential equipment.	24 24

confirm the threefold application value of the proposed novel cooperative layout optimization method:

Firstly, the optimization method can provide superior engineering alternative layout schemes. The original engineering scheme takes into account factors such as stress on nuclear-powered ship pipes and fluid properties, and provides a suboptimal collaborative layout scheme for equipment and pipes. However, upon observation, it was noted that the original scheme excessively emphasized factors such as parallelism between pipes and clamp positions, while neglecting other engineering evaluation factors such as path length and the number of elbows.

Therefore, considering various collaborative factors comprehensively, 30 sets of optimization tests were conducted for both the AA-SPOP algorithm and the excellent DDECS algorithm in this case. The final optimal pipe and equipment

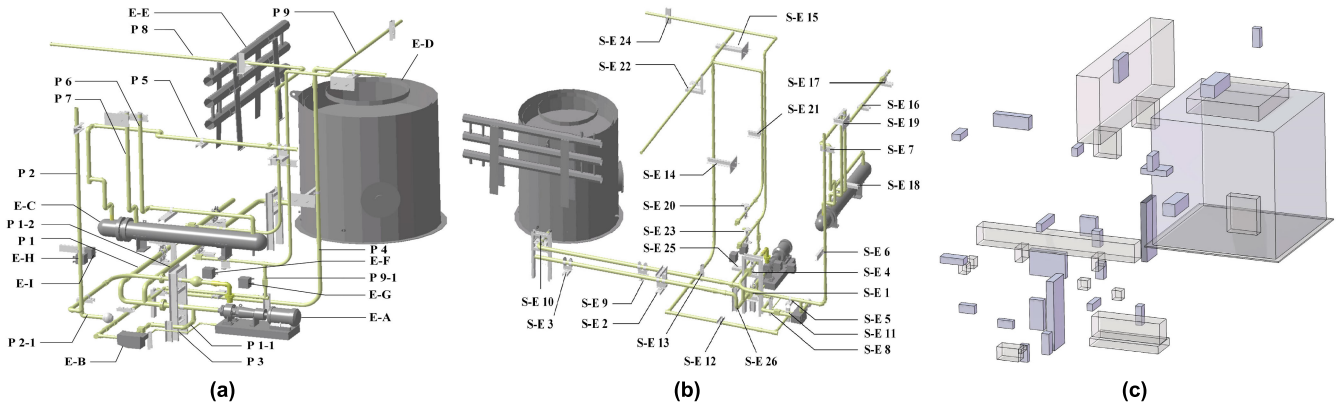

FIGURE 25. Layout space of project Case 3. (a) Original Illustration of pipe and equipment. (b) Original Illustration of support equipment (c) After envelope processing.

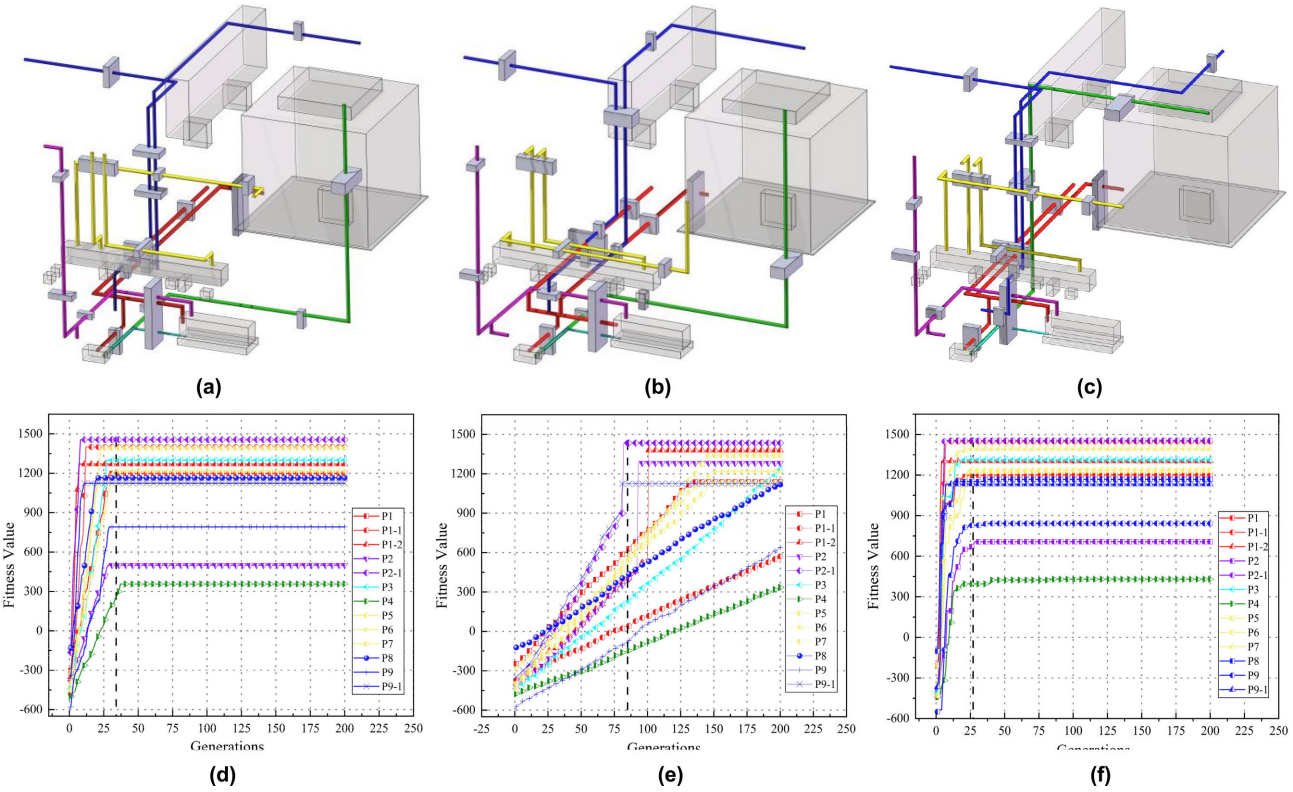

FIGURE 26. Comparison of co-layout results for multi-pipe and equipment (best result). (a) Results of DDECS algorithm. (b) Results of AA-SPOP(G) algorithm. (c) Results of AA-SPOP algorithm. (d) Overall convergence status (DDECS). (e) Overall convergence status (AA-SPOP(G)). (f) Overall convergence status (AA-SPOP).

collaborative layout schemes for each algorithm, as well as algorithm performance, are illustrated in Fig. 26. Table 7 presents a comparison of the data between the new and original layout schemes, where L_v represents the overall path length, E_v represents the number of elbows, P_v represents the parallelism degree of each pipe, P_v_r represents the percentage of parallel length, and B_C represents the degree of change in equipment positions, with 0 indicating that the equipment layout complies with the original engineering plan. If any equipment does not meet the requirements, it is assigned a value of -50.

Based on the comprehensive results, the performance comparison of the algorithms in a large environmental space is as follows: AA-SPOP > DDECS > AA-SPOP(G). Both DDECS and AA-SPOP(G) algorithms exhibit superior layout results compared to the original engineering plan in terms of pipe length and the number of bends. However, they demonstrate reduced parallel collaboration among pipes,

TABLE 7. Comparison of pipe and support equipment collaborative layout results.

Pipe ID	Indicator	Origin	AA-SPOP(G)	DDECS	AA-SPOP
P1 P1-1 P1-2	L_v	132.6	123.5	128.1	124.1
	E_v	9	6	6	6
	P_v	107.3	116.1	114.1	113.1
	P_v_r	81.3%	94.1%	89.2%	91.1%
	B_C	0	+0	+50	+50
P2 P2-1	L_v	79.8	74.7	71.7	73.9
	E_v	6	5	5	5
	P_v	8.0	14.7	14.9	17.6
	P_v_r	9.9%	19.9%	20.8%	23.7%
	B_C	0	-50	-50	0
P3	L_v	18.6	18.6	18.6	18.6
	E_v	3	1	1	1
	P_v	14.0	10.0	10.0	10.0
	P_v_r	74.8%	54.1%	54.1%	54.1%
	B_C	0	0	0	0
P4	L_v	106.3	94.3	94.3	92.3
	E_v	5	2	2	2
	P_v	38.1	11.0	11.0	62.8
	P_v_r	36.1%	12.2%	12.2%	67.9%
	B_C	0	-100	-50	-50
P5	L_v	55.4	46.8	46.8	46.8
	E_v	8	3	2	2
	P_v	14.6	16.0	14.6	14.6
	P_v_r	25.7%	33.8%	30.8%	30.8%
	B_C	0	-50	-50	0
P6	L_v	36.5	36.5	36.5	36.5
	E_v	3	3	3	3
	P_v	18.6	34.5	16.1	18.6
	P_v_r	50.8%	94.1%	44.3%	50.8%
	B_C	0	0	0	0
P7	L_v	20.6	20.6	20.6	20.6
	E_v	2	1	2	1
	P_v	20.6	18.6	18.6	20.6
	P_v_r	100%	90.1%	90.1%	100%
	B_C	0	0	0	0
P8	L_v	87.2	59.4	58.3	58.3
	E_v	3	2	2	2
	P_v	49.3	23.5	34.0	34.0
	P_v_r	56.4%	39.7%	58.2%	58.2%
	B_C	0	0	0	0
P9 P9-1	L_v	104.5	99.6	98.3	97.6
	E_v	6	6	5	6
	P_v	43.4	23.5	34	67.4
	P_v_r	42.3%	24.2%	34.9%	69.2%
	B_C	0	-50	-50	0
Total	L_v	641.5	574.0	573.2	568.7
	E_v	45	29	28	28
	P_v	313.9	267.9	276.7	358.7
	P_v_r	48.9%	46.7%	48.3%	63.1%
	B_C	0	-250	-200	0
Total Change	L_v	-	10.5%	10.6%	11.4%
	E_v	-	35.6%	42.2%	37.8%
	P_v_r	-	-2.2%	-0.6%	14.2%
	B_C	-	-250	-150	0

and the collaborative effects among equipment are relatively suboptimal. In contrast, the AA-SPOP algorithm excels in all aspects of pipe layout, and its collaborative results meet engineering standards. Therefore, this paper's method, while meeting the engineering requirements of the original plan, yields superior overall layout results, reaffirming the efficiency of the new collaborative method and encoding approach.

Secondly, this optimization method has practical value in engineering practice as it can reproduce the original

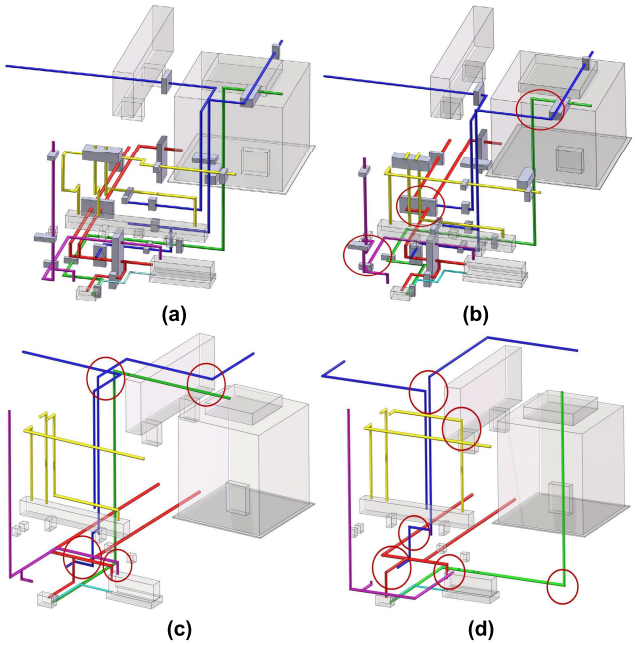

FIGURE 27. Other effects of collaborative approaches (a) Reproducing the original engineering design. (b) Different schemes similar to the original project. (c) Results of hybrid pipe co-layout 1. (d) Results of hybrid pipe co-layout 2.

engineering design and achieve the same layout results. Based on the layout scheme provided in Fig. 25, the collaborative layout optimization method proposed in this paper can be applied to obtain two representative layout results, as shown in Fig. 27. One of them reproduces the original engineering layout as shown in Fig. 27(a), while the other represents a different optimized solution after further optimization as shown in Fig. 27(b). This once again validates the engineering applicability of the proposed collaborative method.

Thirdly, the optimization method exhibits flexibility and diversity in the layout of mixed pipes. Pipe layout holds priority and serves as the foundation for global collaborative optimization. By employing the evaluation Equation (6) and the proposed pipe collaborative optimization method in this study, 30 tests were conducted on Case 3 (Considering only the pipe). By adjusting the different weight parameters in the algorithm, two relatively optimal layout schemes were obtained, as shown in Fig. 27. Fig. 27(c) primarily prioritizes the parallelism between pipes, while Fig. 27(d) prioritizes the overall path length and the number of elbows in the pipes. By increasing the weight parameter $p5$ to a proportion of 0.01 and decreasing $p3$ to a proportion of 0.0005 and $p4$ to a proportion of 0.005, the layout scheme in Fig. 27(c) is obtained. By increasing the weight parameter $p3$ to 0.01 and $p4$ to 0.1, while keeping the others unchanged, the layout scheme in Fig. 27(d) is obtained. The significant differences between these two schemes are clearly visible from the annotated circles in the figures, especially for pipes $P1-1$, $P2$, $P4$, $P5$, $P8$, $P9$, and $P9-1$.

In summary, the collaborative layout method proposed in this paper exhibits strong engineering applicability and

flexibility. In practical scenarios, this method can provide different layout schemes to achieve multiple objectives or emphasize specific goals. Engineers can select the most suitable scheme based on the requirements of the ship.

VI. CONCLUSION

1) Addressing the limitations of traditional grid-based encoding, this paper introduces a flexible high-dimensional vector encoding technique, tailored to the context of ship pipe layout, making significant contributions at the foundational level of the pipe domain.

2) To tackle efficiency, stability, and economic issues within SPRD, a highly versatile heuristic hybrid algorithm, AA-SPOP, is proposed. This algorithm exhibits strong global optimization capabilities and speed. Test results demonstrate the algorithm's high practical value.

3) Addressing the current research gap in pipe collaborative layout, a novel branch pipe layout method is proposed. This method avoids the collaborative deficiencies of traditional approaches, achieving a ''win-win'' arrangement among pipes and paving the way for new research directions.

4) To address the research gap regarding the coordinated layout of pipes and support equipment within ship compartments, this paper, presents a new approach to collaborative layout through mutual guidance of energy zones. Practical ship engineering cases confirm its feasibility and practicality, providing significant reference value for future research in the field of pipe coordination.

In conclusion, this paper has contributed significantly to the fundamental aspects of pipe design, algorithm development, and the collaborative domain, offering novel insights for SPRD. Notably, addressing collaboration issues aligns with the current research mainstream. Future research directions are expected to focus on comprehensive collaborative layouts within ship cabin. Furthermore, there is a need for the development of intelligent ship pipe layout software with practical engineering value.

REFERENCES

[1] M. Palmer and M. Gilbert, *Product Data Representation and Exchange Application Protocol: Plant Spatial Configuration*, Standard ISO/IS 10303-227, International Standards Organization, Jul. 2023.
[2] T. Koch and K. Kreutzer, ''Refactoring early ship design methodologies,'' Atlantec Enterprise Solutions GmbH, Hamburg, Germany, 2017. [Online]. Available: https://www.atlantec-es.com/files/Downloads/Refactoring%20Early%20Ship%20Design%20Methodologies.pdf
[3] W. Wang, F. Zhang, and L. S. Chen, ''Radioactive research on main steam pipe rupture accident of nuclear-powered equipment of ship,'' *Appl. Mech. Mater.*, vols. 152–154, pp. 1729–1735, Jan. 2012.
[4] Y. Ando and H. Kimura, ''An automatic piping algorithm including elbows and bends,'' *J. Jpn. Soc. Nav. Architects Ocean Eng.*, vol. 15, pp. 219–226, Jan. 2012.
[5] J.-G. Min, W.-S. Ruy, and C. S. Park, ''Faster pipe auto-routing using improved jump point search,'' *Int. J. Nav. Archit. Ocean Eng.*, vol. 12, pp. 596–604, Jan. 2020.
[6] S.-H. Kim, W.-S. Ruy, and B. S. Jang, ''The development of a practical pipe auto-routing system in a shipbuilding CAD environment using network optimization,'' *Int. J. Nav. Archit. Ocean Eng.*, vol. 5, no. 3, pp. 468–477, Sep. 2013.
[7] M. Yan, H. Hu, G. Hu, Z. Liu, C. He, and Q. Yi, ''Comparison of heuristic and deterministic algorithms in neutron coded imaging reconstruction,'' *Nucl. Instrum. Methods Phys. Res. A, Accel. Spectrom. Detect. Assoc. Equip.*, vol. 985, Jan. 2021, Art. no. 164704.
[8] W. Yun, ''Intelligent layout optimization design of ship pipe,'' *J. Shanghai Jiaotong Univ.*, vol. 49, no. 4, p. 513, Apr. 2015.
[9] R. Storn and K. Price, ''Differential evolution—A simple and efficient heuristic for global optimization over continuous spaces,'' *J. Global Optim.*, vol. 11, no. 4, pp. 341–359, Jan. 1997.
[10] T. Takimi, ''A study on ant colony optimization,'' *J. Photopolymer Sci. Technol.*, vol. 34, no. 4, pp. 357–362, Jun. 2021.
[11] J. Kennedy and R. Eberhart, ''Particle swarm optimization,'' in *Proc. ICNN Int. Conf. Neural Netw.*, vol. 4, Nov. 1995, pp. 1942–1948.
[12] F. Hemasian-Etefagh and F. Safi-Esfahani, ''Group-based whale optimization algorithm,'' *Soft Comput.*, vol. 24, no. 5, pp. 3647–3673, Mar. 2020.
[13] Z. Dong and X. Bian, ''Ship pipe route design using improved A* algorithm and genetic algorithm,'' *IEEE Access*, vol. 8, pp. 153273–153296, 2020.
[14] W. Niu, H. Sui, Y. Niu, K. Cai, and W. Gao, ''Ship pipe routing design using NSGA-II and coevolutionary algorithm,'' *Math. Problems Eng.*, vol. 2016, pp. 1–21, Jun. 2016.
[15] C. Liu, L. Wu, X. Huang, and W. Xiao, ''Improved dynamic adaptive ant colony optimization algorithm to solve pipe routing design,'' *Knowl.-Based Syst.*, vol. 237, Feb. 2022, Art. no. 107846.
[16] I. I. Aina and C. N. Ejieji, ''Refined heuristic swarm intelligence algorithm,'' *Earthline J. Math. Sci.*, vol. 5, pp. 267–275, Sep. 2020.
[17] X. L. Li, ''A new intelligent optimization-artificial fish swarm algorithm,'' Doctor thesis, Zhejiang Univ. Zhejiang, China, Jan. 2013, vol. 27.
[18] Y. Huang, P. Wang, M. Yuan, and M. Jiang, ''Path planning of mobile robots based on logarithmic function adaptive artificial fish swarm algorithm,'' in *Proc. 36th Chin. Control Conf. (CCC)*, Jul. 2017, pp. 4819–4823.
[19] L. Zhao, Y. Bai, F Wang, and J. Bai, ''Path planning for autonomous surface ships based on improved artificial fish swarm algorithm: A further study,'' *Ships Offshore Struct.*, vol. 6, pp. 897–906, Sep. 2022.
[20] Y. Wang, H. Wei, G. Guan, K. Li, Y. Lin, and S. Chai, ''Intelligent layout design of ship pipeline using a particle swarm optimisation integrated genetic algorithm,'' *Int. J. Maritime Eng.*, vol. 163, no. 2, Jul. 2021.
[21] Y. Lin and Q. Zhang, ''A multi-objective cooperative particle swarm optimization based on hybrid dimensions for ship pipe route design,'' *Ocean Eng.*, vol. 280, Jul. 2023, Art. no. 114772.
[22] P. Lu, L. Ye, Y. Zhao, B. Dai, M. Pei, and Y. Tang, ''Review of meta-heuristic algorithms for wind power prediction: Methodologies, applications and challenges,'' *Appl. Energy*, vol. 301, Nov. 2021, Art. no. 117446.
[23] M. Henderson and T. D. Ngo, ''RRT-SMP: Socially-encoded motion primitives for sampling-based path planning,'' in *Proc. 30th IEEE Int. Conf. Robot Hum. Interact. Commun. (RO-MAN)*, Aug. 2021, pp. 330–336.
[24] J.-P. Heo, Z. Lin, and S.-E. Yoon, ''Distance encoded product quantization for approximate K-nearest neighbor search in high-dimensional space,'' *IEEE Trans. Pattern Anal. Mach. Intell.*, vol. 41, no. 9, pp. 2084–2097, Sep. 2019.
[25] Y. Yu, Z. Ji, J. Guo, and Z. Zhang, ''Zero-shot learning via latent space encoding,'' *IEEE Trans. Cybern.*, vol. 49, no. 10, pp. 3755–3766, Oct. 2019.
[26] Z. Lin, G. Ding, J. Han, and L. Shao, ''End-to-end feature-aware label space encoding for multilabel classification with many classes,'' *IEEE Trans. Neural Netw. Learn. Syst.*, vol. 29, no. 6, pp. 2472–2487, Jun. 2018.
[27] A. Asmara, *Pipe Routing Framework for Detailed Ship Design*. Delft, The Netherlands: TUD Technische Universiteit Delft, 2013, p. 155.
[28] Q. Liu and C. Wang, ''Multi-terminal pipe routing by Steiner minimal tree and particle swarm optimisation,'' *Enterprise Inf. Syst.*, vol. 6, no. 3, pp. 315–327, Aug. 2012.
[29] G. Guan, Y. Lin, and Y. Chen, ''An optimisation design method for cryogenic pipe support layout of LNG-powered ships,'' *J. Mar. Eng. Technol.*, vol. 16, no. 1, pp. 45–50, Jan. 2017.
[30] Y. Wang, H. Wei, X. Zhang, K. Li, G. Guan, C. Jin, and L. Yan, ''Optimal design of ship branch pipe route by a cooperative co-evolutionary improved particle swarm genetic algorithm,'' *Mar. Technol. Soc. J.*, vol. 55, no. 5, pp. 116–128, Sep. 2021.
[31] Y. Xu, L. Zhang, H. Wei, Z. Zhang, F. Yang, H. Hu, and Y. Hu, ''Nonlinear dynamics of viscoelastic fluid-conveying pipe installed within uniform external cross flow by pipe clamps,'' *Appl. Ocean Res.*, vol. 135, Jun. 2023, Art. no. 103547.
[32] A. Asmara, U. Nienhuis, and R. Hekkenberg, ''Approximate orthogonal simplification of 3D model,'' in *Proc. IEEE Congr. Evol. Comput.*, Jul. 2010, pp. 1–4.

[33] Z.-R. Dong, X.-Y. Bian, and S. Zhao, "Ship pipe route design using improved multi-objective ant colony optimization," *Ocean Eng.*, vol. 258, Aug. 2022, Art. no. 111789.
[34] Y. Lin, X. Bian, and Z. Dong, "Ship pipe layout optimization based on improved particle swarm optimization," *J. Shanghai Jiaotong Univ. Sci.*, vol. 28, pp. 1–10, Nov. 2022.
[35] H. Sui and W. Niu, "Branch-pipe-routing approach for ships using improved genetic algorithm," *Frontiers Mech. Eng.*, vol. 11, no. 3, pp. 316–323, May 2016.
[36] J. Heo, Y. H. Jang, and S. Baek, "Optimum positioning of friction support for vibration reduction in piping system," *The J. Acoust. Soc. Korea*, vol. 41, no. 6, pp. 680–690, Nov. 2022.
[37] K. Kishida and M. Yamadera, "Optimization for pipe support locations," *Ishikawajima-Harima Giho*, vol. 30, no. 4, pp. 230–233, 1990.
[38] J. Lin, Y. Zhao, Q. Zhu, S. Han, H. Ma, and Q. Han, "Nonlinear characteristic of clamp loosing in aero-engine pipeline system," *IEEE Access*, vol. 9, pp. 64076–64084, 2021.
[39] X. Li, L. Zhang, S. Wang, and C. Zhang, "Impedance analysis and clamp locations optimization of hydraulic pipeline system in aircraft," in *Proc. Int. Conf. Fluid Power Mechatronics (FPM)*, Aug. 2015, pp. 1034–1039.
[40] Y. Lin, X.-Y. Bian, and Z.-R. Dong, "A discrete hybrid algorithm based on differential evolution and cuckoo search for optimizing the layout of ship pipe route," *Ocean Eng.*, vol. 261, Oct. 2022, Art. no. 112164.
[41] W.-Y. Jiang, Y. Lin, M. Chen, and Y.-Y. Yu, "A co-evolutionary improved multi-ant colony optimization for ship multiple and branch pipe route design," *Ocean Eng.*, vol. 102, pp. 63–70, Jul. 2015.

HONGSHUO ZHANG was born in Tangshan, Hebei, China, in June 2000. He received the B.S. degree in navigation technology from Shanghai Maritime University, in July 2022. He is currently pursuing the M.S. degree in design and manufacture of ships and marine structures with the Dalian University of Technology. His main research interests include automatic layout optimization of ship piping systems, optimization algorithms, and intelligent ships. He has made significant contributions to this research field through the publication of core papers and patents. Additionally, he has achieved numerous awards in national-level competitions, such as the National Marine Ship Design and Construction Competition and the Mathematical Modeling Competition.

MINGJUN YANG was born in Chaoyang, Liaoning, in 1999. He received the B.S. degree in maritime management from Dalian Maritime University, in July 2021. He is currently pursuing the M.S. degree in ship and marine structure design and manufacturing with the Dalian University of Technology. His research interests include the automatic laying of ship pipes and ship route planning. He has published core papers and soft works. He has won many awards in mathematical modeling competitions, programming competitions, and national postgraduate smart city competitions. He has won many national awards.

YUANSONG YANG was born in 1981. He is currently a Senior Engineer and has been the Deputy Director of the Key Laboratory of Science and Technology on Green Construction, China Nuclear Industry 23 Construction Company Ltd. His research interests include nuclear engineering BIM technology, digital technology, and intelligent equipment. Over the past decade, he has published numerous papers and patents in this field, producing valuable results that have been widely utilized. He has also led or participated in several national and provincial research projects.

HAIYANG LIU was born in 1985. He is currently an Associate Senior Engineer and has been the Executive Director of the Key Laboratory of Science and Technology on Green Construction, China Nuclear Industry 23 Construction Company Ltd. His research interests include nuclear engineering BIM technology, digital technology, and virtual design. He has participated in numerous national and provincial research projects and has achieved extensive research outcomes.

YAN LIN received the B.S. and M.S. degrees in ship and ocean engineering from the Dalian University of Technology, China, in 1984 and 1987, respectively, and the Ph.D. degree in design and manufacture of ships and marine structures from Shanghai Jiao Tong University, China, in 1993. He is currently a Professor and a Ph.D. Supervisor with the Dalian University of Technology and a member of the Sixth and Seventh Discipline Assessment Committees of the Academic Degrees Committee of the State Council. His main research interests include the development of intelligent ships, unmanned specialized ships, ship virtual collaboration and digital design technology, and key technologies for overall design of marine platforms. He has authored 11 academic monographs and eight textbooks. He has published 430 papers in domestic and international academic journals and conferences (including 265 papers indexed by SCI, EI, ISTP, and BMT), and holds 27 international patents. He has won multiple national honors.